# MOBILITY EXERCISE A (MEXA) FIELD TEST PROGRAM. REPORT 4. PERFORMANCE OF SELECTED MEXA AND MILITARY VEHICLES IN VERTICAL OBSTACLES

Army Engineer Waterways Experiment Station,
Vicksburg, Mississippi

January 1974

[redacted]

[redacted]

The findings in this report are not to be construed as an official Department of the Army position unless so designated by other authorized documents.

TECHNICAL REPORT M-70-11

# MOBILITY EXERCISE A (MEXA) FIELD TEST PROGRAM

Report 4

## PERFORMANCE OF SELECTED MEXA AND MILITARY VEHICLES IN VERTICAL OBSTACLES

by

N. R. Murphy, Jr., A. A. Rula

January 1974

Sponsored by U. S. Army Materiel Command, Washington, D. C.
Project Nos. 1T162112A131 and 1T162112A046, Task 02

Conducted by U. S. Army Engineer Waterways Experiment Station
Mobility and Environmental Systems Laboratory
Vicksburg, Mississippi

THE CONTENTS OF THIS REPORT ARE NOT TO BE USED FOR ADVERTISING, PUBLICATION, OR PROMOTIONAL PURPOSES. CITATION OF TRADE NAMES DOES NOT CONSTITUTE AN OFFICIAL ENDORSEMENT OR APPROVAL OF THE USE OF SUCH COMMERCIAL PRODUCTS.

## FOREWORD

The study reported herein was performed by the U. S. Army Engineer Waterways Experiment Station (WES) for the U. S. Army Materiel Command (AMC) and is part of the Mobility Exercise A (MEXA) program to evaluate the performance of three new vehicle concepts relative to the performance of three military vehicles. Funds for the MEXA program were provided under Projects 1T162112A131, "Environmental Constraints on Materiel" and 1T162112A046, "Trafficability and Mobility Research," Task 02, "Surface Mobility."

This study was conducted in August-October 1968 by personnel of the Mobility Systems Division (MSD) under the general supervision of Messrs. W. G. Shockley, Chief, Mobility and Environmental Systems Laboratory (MESL), S. J. Knight, former Assistant Chief, MESL, and A. A. Rula, Chief, MSD. Planning and execution of field tests were under the general direction of Mr. J. K. Stoll, formerly of MSD. Major assistance was given in analog computer analysis by Mr. G. G. Switzer, MSD, and in digital computer analysis by Mr. J. F. Smith, formerly of the Automatic Data Processing Center. The data were analyzed by Mr. N. R. Murphy, Jr., (MSD) and the report was prepared by Messrs. Murphy and Rula. Appendix A was prepared by Mr. Murphy.

This report is one in a series entitled "Mobility Exercise A (MEXA) Field Test Program." Other reports in the series are as follows: Report 1, "Summary"; Report 2, "Performance of the MEXA and Three Military Vehicles in Soft Soils"; Report 3, "Performance of the MEXA and Three Military Vehicles in Lateral Obstacles"; and Report 5, "Performance of Selected MEXA and Military Vehicles in Selected Natural Terrains." Reports 1 and 5 have not yet been published.

Directors of the WES during the conduct of this study and preparation of the report were COL John R. Oswalt, Jr., CE, COL Levi A. Brown, CE, BG Ernest D. Peixotto, CE, and COL G. H. Hilt, CE. Technical Directors were Messrs. J. B. Tiffany and F. R. Brown.

CONTENTS

## CONVERSION FACTORS, BRITISH TO METRIC UNITS OF MEASUREMENT

British units of measurement used in this report can be converted to metric units as follows:

| Multiply | By | To Obtain |
|---|---|---|
| inches | 2.54 | centimeters |
| feet | 0.3048 | meters |
| miles (U. S. statute) | 1.6093 | kilometers |
| pounds | 0.4536 | kilograms |
| pounds per square inch | 6.8948 | kilonewtons per square meter |
| tons (short) | 0.9072 | metric tons |

## SUMMARY

Fifty tests were conducted with two vehicles, an XM410E1, 8x8, 2-1/2-ton cargo truck and the MEXA 10x10, 2-1/2-ton, wheeled, articulated test bed. The vertical obstacle test course at WES, on which rigid, single or multiple obstacles of various heights and shapes can be tested, was used. The primary purpose of these tests was to obtain data to relate obstacle height, vehicle speed, and vertical acceleration (at selected locations on the vehicle) for use as input to the AMC-71 cross-country mobility prediction model. A secondary purpose was to provide data for use in verifying the vehicle dynamics prediction models using test data for the XM410E1 and MEXA 10x10. Results of the test are presented by curves relating, for a series of obstacle heights, the speed of the vehicle at contact with the obstacle versus peak accelerations at selected locations on the vehicle, and obstacle height versus speed for a vertical acceleration of 2.5 g's in the driver's compartment and vehicle center of gravity. Test data are compared with predicted results obtained from the dynamic response computer models for both vehicles.

The results indicate among other things that: (a) the intensity of vertical acceleration depends on the location in the vehicle; (b) human tolerance levels are reached only for vertical accelerations; (c) tire pressure can significantly affect peak acceleration relations; (d) for a given level of acceleration, speed decreases with an increase in obstacle height; and (e) with proper input the mathematical models can be used to adequately simulate speed-obstacle height relations.

It is recommended that additional data be obtained for a variety of vehicle types to establish experimental speed-obstacle height relations to determine if peak vertical accelerations and obstacle heights are suitable quantities for defining obstacle-crossing capabilities, and to validate the current models that simulate dynamic response.

# MOBILITY EXERCISE A (MEXA) FIELD TEST PROGRAM
# PERFORMANCE OF SELECTED MEXA AND MILITARY VEHICLES IN VERTICAL OBSTACLES

## PART I: INTRODUCTION

### Background

1. Discrete, vertical obstacles that do not cause vehicle immobilizations but do produce shock motions to the driver-vehicle-cargo system have a significant effect on the speed at which a vehicle can cross an obstacle or override irregular terrain. The forces generated by the sudden impact of a moving vehicle with a discrete obstacle can cause serious injury to the driver and/or damage to the vehicle and cargo. Therefore, when vertical obstacles large enough to produce shocks must be overridden, a driver reacts by slowing his vehicle to a speed he considers commensurate with his own safety and comfort and the safety of his vehicle or cargo.

2. Measurements made at the driver's seat during cross-country tests show that a driver will attempt to regulate the speed of his vehicle to avoid being subjected to peak vertical and longitudinal accelerations in excess of approximately 2.5 and 2.0 g, respectively. A consistency of driver reaction to this self-imposed tolerance limit has been established by results of cross-country tests conducted by the U. S. Army Engineer Waterways Experment Station (WES) with a variety of vehicles and drivers in Thailand[1] and Nevada,[2] and by data reported by Cardwell[3] on cross-country tests conducted by the Ministry of Defense, United Kingdom.

3. Available measurements of vertical acceleration at the driver's seat show that the number of occurrences exceeding 2.5 g's is comparatively small. The relatively small number of occurrences per mile of acceleration magnitudes in the 2- to 3-g range for all tests is thought to be related to the driver's tendency to control dynamic responses by regulating the speed of his vehicle.

4. Based on the above test results and observations, the values of 2.5-g peak vertical acceleration and 2.0-g peak longitudinal acceleration have been accepted by WES as human tolerance criteria for establishing maximum obstacle-traversal speeds. No consideration is given to the sign of the acceleration, since +2.5 g's appear to have the same effect on the driver as -2.5 g's. Therefore, in this report, reference to peak accelerations refers to the largest numerical value regardless of sign.

5. The plan for the Mobility Exercise A (MEXA) field tests consisted of a four-phase program. During phase I speed performance was evaluated for a range of soil strengths, from the immobilization point of the three MEXA vehicles and three military vehicles up to and including a hard-surface road; phase II included establishing engineering performance characteristics and essential terrain-vehicle relations; phase III included a refinement or improvement of the terrain-vehicle relations required by the WES cross-country speed prediction model;* and phase IV included testing the reliability of the updated cross-country speed prediction model, using as input the relations obtained during actual field testing of the three MEXA and three military vehicles. The tests reported herein were conducted during phase III.

## Purpose

6. The primary purpose of the tests was to obtain data for establishing relations among obstacle height, vehicle speed, and vertical and longitudinal accelerations for use as input to the cross-country speed prediction model. A secondary purpose was to obtain experimental data to verify the WES wheeled vehicle dynamics prediction models.

## Scope

7. A total of 50 tests were conducted with an XM410E1 wheeled

---

* As a result of the developments of a joint effort initated in August 1970 between the U. S. Army Tank-Automotive Command and WES, this model evolved into what is now referred to as the AMC-71 Ground Mobility Model.

military vehicle and the MEXA 10x10 wheeled test bed over single, rigid, half-round obstacles ranging in height from 4 to 12 in.* The obstacles were secured to a smooth, level, firm surface. Test speeds ranged from 2.25 to 21.27 mph. Measurements of peak vertical and longitudinal accelerations and impact speed (the speed at which the vehicle first encounters the obstacle) were related to obstacle height and driver tolerance criteria. Test results were compared with dynamic response of the vehicles predicted by analog and digital computer models. These models are described in Appendix A.

8. The number and scope of the tests were held to a minimum because of the limited time and funds available for this phase of the overall study. Structural damage to the MEXA 10x10 sustained in other tests further limited the scope of testing with this vehicle.

---

* A table of factors for converting British units of measurement to metric units is given on page ix.

## PART II: FIELD TEST PROGRAM

### Location and Description of Test Course

9. A permanent, level, vertical-obstacle test course (fig. 1) located on the WES reservation was used for this study. The course consists of two parallel, 200-ft-long, paved strips spaced to accommodate a variety of vehicle widths. Adjacent to the outer edges of the paved strips are U-shaped concrete grade beams with 8-in.-wide, 3/8-in.-thick steel plate covers. The covers are welded to 6-in. channels embedded in the top of the beams and are slotted to allow for bolting single or multiple obstacles in desired position(s). Only single obstacles were used in this study.

### Test Equipment

#### Test vehicles

10. The test vehicles were an XM410E1, 8x8, 2-1/2-ton cargo truck and the MEXA 10x10, 2-1/2-ton, wheeled, two-unit articulated test bed (fig. 2). The general vehicle characteristics pertinent to this study are listed in table 1. Specific vehicle data required as input to the vehicle dynamic response models are presented in table A1 (Appendix A) for the XM410E1 and in paragraph 7 of Appendix A for the MEXA 10x10 vehicle.

#### Instrumentation

11. The following transducers were used to measure test data.

a. One 10-g servo-accelerometer oriented in the vertical plane and located adjacent to and below the left side of the driver's seat on the XM410E1 (space was not available under the driver's seat), and one oriented in the vertical plane and mounted directly below the driver's seat on the 10x10 test bed to measure the vertical accelerations at the drivers' seats.

Fig. 1. WES vertical-obstacle test course


a. 2-1/2-ton XM410E1, 8x8, cargo truck

Fig. 2. Test vehicles

b. 2-1/2-ton MEXA 10x10 test bed

b. One 10-g servo-accelerometer oriented in the vertical plane and one 5-g servo-accelerometer oriented in the longitudinal plane, mounted as close as possible to the center of gravity of each vehicle, to measure vertical and longitudinal acceleration at the center of gravity.

c. One 25-g strain-gage accelerometer oriented in the vertical plane, mounted on the left_front axle of the XM410E1, to measure vertical acceleration at the axle.

d. A tachometer device, mounted on the rear deck of each vehicle, to measure vehicle speed and the distance traveled.

e. A telemetering torque sensor, mounted on the torsional coupling between the transmission and transfer case of the XM410E1, to measure tractive force.

12. The recording system consisted of a light-beam oscillograph and magnetic tape recorder installed in an instrumentation van and connected to the transducers on the test vehicle by an umbilical-type cable.

13. Instrumentation installed on the test vehicles provided continuous measurements of longitudinal and vertical accelerations, vehicle speed, horizontal distance, and, for the XM410, drive-line torque. These data, together with the 0.1-sec timing lines indicated on the record and event marks to indicate camera reset, frame count, and contact of each set of wheels with the obstacle, were recorded by the oscillograph and the magnetic tape recorders. The event marks indicating wheel contact with the obstacle for each axle were recorded on the same channel with the distance measurements. An oscillogram for a test (item 8, table 2) conducted with the XM410E1 at 5.35 mph over a 6-in. obstacle is shown in fig. 3.

14. Additional instrumentation and recording equipment included a high-speed 35-mm camera to record vehicle motions and attitudes during the tests for qualitative evaluations. It was mounted at distances of

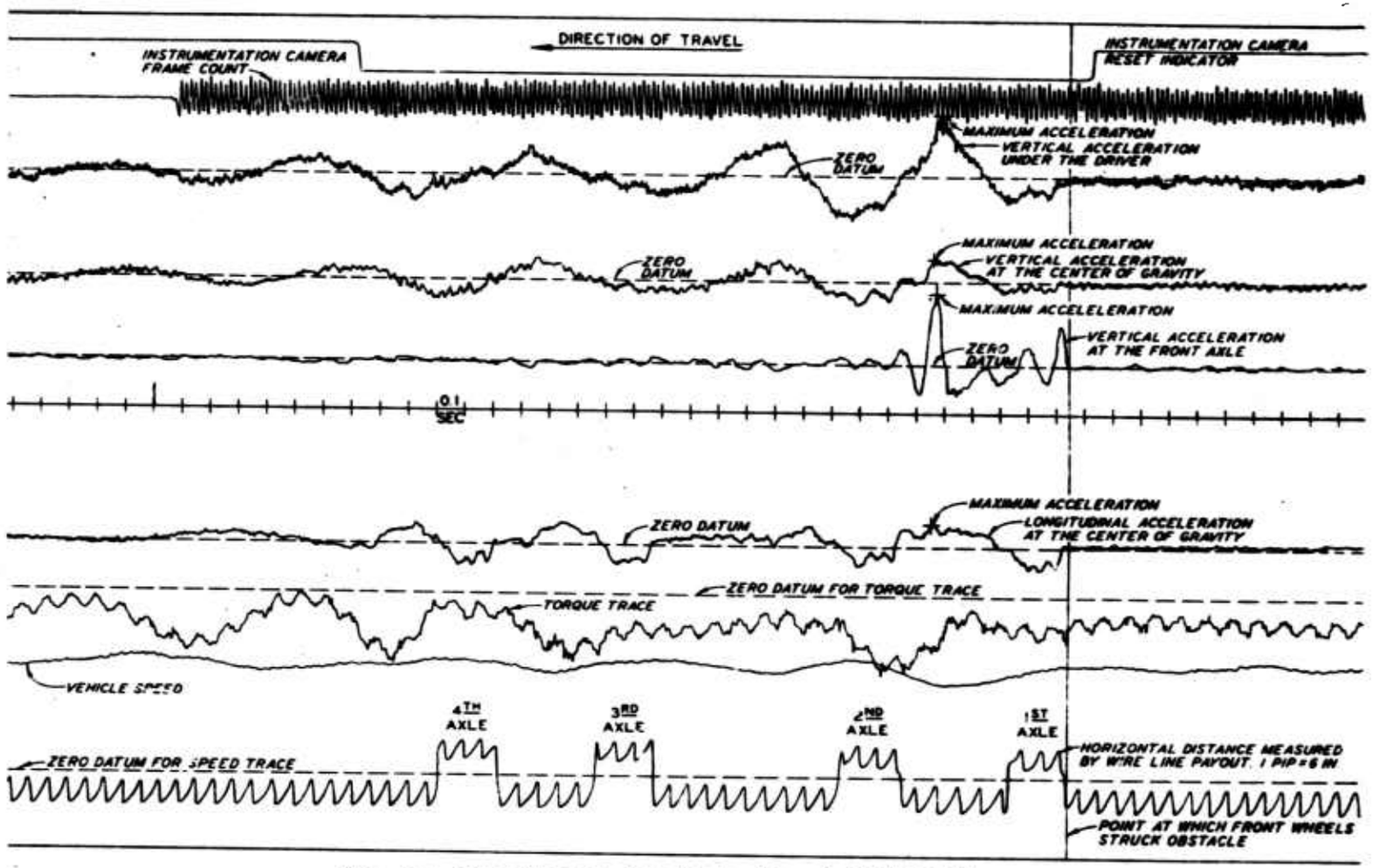


Fig. 3. Oscillogram for test item 8 (XM410E1)

25 and 50 ft from the obstacle being tested, on a line perpendicular to the test course and with the lens at an elevation equal to that of the hub on the front axle of the vehicle in static position, and was operated at a film speed of 57 frames per second.

## Tests

15. The following 50 tests were conducted to establish relations among vehicle dynamic response, vehicle speed, and obstacle height.

| Test Vehicle | No. of Tests | Tire Inflation Pressure psi | Obstacle Height in. | Range of Vehicle Speed mph |
|---|---|---|---|---|
| XM410E1 | 5 | 20 | 6 | 2.90- 9.25 |
| | 5 | (18.2%* average | 8 | 2.60- 9.20 |
| | 3 | deflection) | 10 | 2.30- 5.50 |
| | 2 | | 12 | 2.50- 3.85 |
| | 5 | 10-15** | 6 | 2.80- 9.05 |
| | 5 | (25% deflection) | 8 | 2.25- 9.75 |
| | 2 | | 10 | 2.35- 3.95 |
| 10x10 | 4 | 9 | 4 | 5.80-21.75 |
| | 16 | | 6 | 2.90-19.10 |
| | 3 | | 8 | 3.50- 7.15 |

16. The test vehicle was positioned at one end of the test course at a distance from the obstacle sufficient to permit the driver to reach the required test speed at a designated point on the course. Before the start of each test run, calibrations for the measurement system were

---

* Percent deflection is equal to the tire deflection divided by tire section height times 100. For 20-psi tire-inflation pressure, individual tire deflections ranged from 15.6 to 20.3 percent. The average deflection of 18.2 percent for all eight tires gave a mean deviation of 0.96. For the two front tires, which were most significant in the analysis of the test data, percent deflections were 18.1 and 17.8 for the left and right tires, respectively.

** The range of inflation pressures required to obtain 25 percent tire deflection of each tire.

recorded as required. The driver attained the required test speed prior to arriving at a marker placed about 10 ft in front of the obstacle. He then attempted to hold the vehicle speed constant while crossing the obstacle and for a distance of approximately 1-1/2 vehicle lengths beyond the obstacle to allow for measurement of residual motions. All obstacles were encountered perpendicularly to the longitudinal axis of the vehicle.

## PART III: ANALYSIS OF DATA

17. The data collected in this test program were analyzed to develop pertinent acceleration-obstacle height-speed relations required to characterize dynamic vehicle response. Similar relations were predicted by mathematical models that simulate dynamic response. The measured and predicted relations were compared to evaluate the prediction accuracy of the models used. Sufficient data were also collected to examine the effect of tire pressure on dynamic response.

### Method of Analysis

18. From a study of the results of dynamic performance of vehicles crossing discrete, rigid obstacles reported herein and in other studies, obstacle height was determined to be the best single descriptor to represent the obstacle in the analysis. Peak vertical and longitudinal accelerations were chosen to describe vehicle dynamic response at several locations within the vehicle, i.e. at the driver's seat, the center of gravity, and the front axle. These peak values are easily determined from oscillograms (fig. 3) and from computer simulations, thus providing a straightforward and simple means for describing vehicle response as a function of speed and obstacle height. With an assumption that vehicle dynamic response is a function of location within the vehicle, height of the obstacle, and impact speed, relations of peak accelerations versus speed were sought from data measured for selected obstacle heights and at the above-mentioned locations within a vehicle. From these relations, obstacle height-speed relations were developed for established driver tolerances (paragraph 2) of vertical and longitudinal accelerations as required as input to the AMC-71 model. The mathematical models described in Appendix A were used to simulate vehicle dynamic response at locations in the vehicle corresponding to those at which responses were measured, and for the obstacle heights and speeds at which tests were run. The predicted data were used to develop the same relations identified above.

## Acceleration-Obstacle Height-Speed Relations Developed from Measured Data

19. The measured data from which acceleration-obstacle height-impact speed relations were developed are listed in table 2. For the XM410E1 truck, separate relations were developed for peak vertical accelerations at the driver's seat, the center of gravity, and the front axle, and for peak longitudinal acceleration at the center of gravity. Similar relations were developed for the MEXA 10x10 test bed, except none were derived for the front-axle location. The acceleration and speed data in table 2 were plotted for specific obstacle heights, and lines of best visual fit were drawn through the data points. From these relations, data were obtained to develop obstacle height-speed relations for established driver tolerance levels of acceleration for both vehicles. The specific relations developed are discussed in the following paragraphs.

### Peak vertical acceleration-speed relations

20. XM410E1. Peak vertical acceleration-speed relations for the XM410E1 truck at the driver's seat, the center of gravity, and the front axle are given in figs. a, b, and c, respectively, of plate 1 for 20-psi tire pressure or an average tire deflection of 18.2 percent. Separate curves are shown for 6-, 8-, 10-, and 12-in.-high obstacles. The scatter in the data is largely attributable to the inability of the driver to strike the obstacle exactly at right angles and maintain a desired speed while the vehicle crossed the obstacle.

21. An examination of the relations presented in plate 1 shows that the magnitude of the vertical acceleration depends on location of the point of dynamic activity considered, the height of the obstacle, and the speed at which the vehicle crosses the obstacle. Vertical acceleration at a given speed and obstacle height was greatest at the front axle (unsprung mass) (fig. c), smallest at the center of gravity (fig. b), and intermediate at the driver's position (fig. a). At all positions, vertical acceleration increased at a given speed with an increase in obstacle height and with an increase in speed for a given obstacle height, except

for the center-of-gravity position and the 6-in. obstacle. In this latter case there appears to be a trend for vertical acceleration to reach a maximum or even decrease at the higher speeds. The relations for the front axle are nearly linear, with the slopes of the curves dependent on obstacle heights. The relations for the driver's seat and center of gravity, which are located in the sprung mass of the vehicle, show much larger increases in vertical acceleration at a given speed between the 8- and 10-in.-high obstacles than between any other two curves separated by a difference of 2 in. in obstacle height.

22. The observed effects indicate that the shape of peak vertical and longitudinal acceleration-impact speed curves (discussed later) is dependent upon tire/obstacle envelopment characteristics, the obstacle height-wheel geometry, impact speed, and vehicle mass. According to the principles of basic mechanics, these factors control the direction and magnitude of the impulse generated in crossing discrete, rigid obstacles.

23. MEXA 10x10. Peak vertical acceleration-speed relations at the driver's seat and center of gravity (front unit) in the MEXA 10x10 test bed are given in figs. a and b, respectively, of plate 2, for 9-psi tire pressure or an average tire deflection of 16.9 percent. Relations are shown for 4-, 6-, and 8-in.-high obstacles. Because of apparent vehicle structural damage, tests could not be run over the 10- and 12-in.-high obstacles, and speed over the 8-in.-high obstacle was limited to about 7 mph.

24. The results indicate the same general trends as those for the XM410E1 truck, i.e. the peak vertical accelerations increased with an increase in speed or obstacle height. As expected, the vertical acceleration was greater at the driver's seat than at the center of gravity. At both locations vertical acceleration for the 4-in.-high obstacle leveled off and then decreased at the higher speeds. At the center of gravity, the curves for the three obstacle heights are fairly evenly spaced with respect to each other. For the 4-in.-high obstacle, the maximum

peak vertical acceleration was reached at about 16 mph, and for the 6-in.-high obstacle it was approached at about 20 mph. At the driver's seat, the maximum peak vertical accelerations for the 4- and 6-in.-high obstacles appear to have been reached at about 17 mph.

Peak longitudinal acceleration-speed relations

25. XM410E1. Peak longitudinal acceleration-speed relations at the center of gravity of the XM410E1 truck are given in fig. a of plate 3, for 20-psi tire pressure. Separate curves are shown for 6-, 8-, 10-, and 12-in.-high obstacles. Peak longitudinal accelerations were considered only at the center of gravity, because the longitudinal axis is not significantly influenced by pitch motion and the magnitude of these accelerations are essentially constant throughout the vehicle. Therefore, the longitudinal accelerations at the center of gravity would be similar to those measured at the driver's seat.

26. The relation shown in plate 3a for the 6-in.-high obstacle is obviously erroneous when it is compared with the relations for the other obstacles. The data from which this curve was drawn are widely scattered. Excluding the 6-in.-obstacle relation, the peak longitudinal acceleration increased in a logical manner with obstacle height and speed. Speed had little or no effect on the acceleration for the 8-in.-high obstacle. When obstacle height approached about 10 in., the obstacle-wheel geometry was such that peak longitudinal acceleration for the XM410E1 type of suspension was apparently affected by obstacle height and speed. For the 12-in.-high obstacle, the rate of change in peak longitudinal acceleration with speed was quite large. The tests were stopped before the longitudinal driver tolerance limit of 2 g's was reached to avoid possible structural damage to the vehicle or bodily injury to the driver due to excessive vertical accelerations.

27. MEXA 10x10. Peak longitudinal acceleration-speed relations for the MEXA 10x10 test bed at the center of gravity are given in fig. b of plate 3, for 9-psi tire pressure. Separate curves are shown for 4-, 6-, and 8-in.-high obstacles.

28. Except for the 4-in.-high obstacle, the data appear to be fairly well scattered. Although the relations were drawn so that peak longitudinal acceleration increased at a given speed with an increase in obstacle height and with an increase in speed for a given obstacle height, it is quite possible that this apparent scatter or dip in the trend noted for the 6- and 8-in.-high obstacles is really the result of the physics of the obstacle-speed-articulated vehicle system. For a given speed, the change in peak longitudinal acceleration was greater between 4- and 6-in.-high obstacles than between 6- and 8-in.-high obstacles.

29. The tendency for accelerations to reach a peak as evidenced by some of the vertical acceleration-speed relations is also apparent for some of the longitudinal acceleration-speed relations. This is indicated by the XM410E1 relations for the 8-in.-high obstacles in fig. a, of plate 3, and the MEXA 10x10 relations for 4- and 6-in.-high obstacles in fig. b of plate 3, which appear to be approaching a peak at the higher speeds.

Obstacle height-speed relations

30. One form of relation that is used to characterize vehicle dynamic response to discrete, rigid obstacles is that of obstacle height versus the maximum speed at which selected peak values of vertical and longitudinal accelerations are not exceeded. As previously stated, driver tolerance limits have been established as 2.5 and 2.0 g's for peak vertical and longitudinal accelerations, respectively. Since the vertical acceleration limit is usually reached before the longitudinal limit, obstacle height-speed relations at which 2.5 g's will occur have been used to characterize vehicle dynamic response to discrete obstacles.

31. For selected values of vertical acceleration, the speeds and obstacle heights at which a given value of acceleration occurred were read for the driver's position from the curves given in plates 1a and 2a for the XM410E1 truck and MEXA 10x10 test bed, respectively. The data obtained in this manner are given in the following tabulation.

| XM410E1 Truck 20-psi Tire Pressure | | MEXA 10x10 Test Bed 9-psi Tire Pressure | |
|---|---|---|---|
| Obstacle Height, in. | Speed, mph | Obstacle Height, in. | Speed, mph |
| | 2.5-g Acceleration | | |
| 8 | 9.2 | 6 | 6.7 |
| 10 | 4.4 | 8 | 5.3 |
| 12 | 3.7 | - | - |
| | 2.0-g Acceleration | | |
| 8 | 7.3 | 4 | 17.5 |
| 10 | 3.8 | 6 | 5.3 |
| 12 | 3.2 | 8 | 4.7 |
| | 1.5-g Acceleration | | |
| 6 | 7.2 | 4 | 7.9 |
| 8 | 5.5 | 6 | 4.3 |
| 10 | 3.2 | 8 | 3.9 |
| 12 | 2.8 | - | - |
| | 1.0-g Acceleration | | |
| 6 | 5.0 | 4 | 5.2 |
| 8 | 4.1 | 6 | 3.5 |
| 10 | 2.6 | 8 | 3.2 |
| 12 | 2.4 | - | - |

The above data for several levels of vertical acceleration are plotted in figs. a and b of plate 4; the curves were drawn on the basis of best visual fit. From the curves it can be seen that at a given level of vertical acceleration, speed decreases with an increase in obstacle height. A comparison of the curves indicates that for a given speed and obstacle height, vertical acceleration is less for the XM410E1 than for the MEXA 10x10 test bed.

## Effects of Tire Pressure on Vertical Acceleration

32. In the case of a vehicle crossing a discrete, rigid obstacle at tire pressures that will produce a hard or a soft tire, the magnitude of the motions produced in the vehicle will be less when it is equipped with soft tires. A soft tire will, to some extent, envelop the obstacle upon contact and will lessen the shock impact on contact with the ground on the other side of the obstacle. Thus, tire pressure influences the magnitude of the bounce and pitch motions and impact force involved in crossing an obstacle. The effects of tire pressure were examined by comparing peak vertical acceleration-speed relations at the center of gravity of the XM410E1 truck for two tire pressures. These relations are shown in plate 5. Although this is by no means a comprehensive analysis, the decreasing rates at which the peak accelerations vary with impact speed indicate that tire pressure may significantly influence peak vertical acceleration, depending on obstacle height and speed. At the low speed, the differences are very small. Generally, as speed increased, the difference in the effect of tire pressure increased, with the lower tire pressure producing lower values of peak vertical acceleration.

## Acceleration-Obstacle Height-Speed Relations Developed from Predicted Data

33. Predicted data for dynamic response of the two test vehicles crossing single, rigid obstacles were obtained by using mathematical models that simulate vehicle-obstacle performance. The XM410E1 truck was simulated with a digital computer model, and the MEXA 10x10 test bed with an analog computer model. These models are discussed in detail in Appendix A. The predicted responses were obtained for both vehicles by successive "runs" over selected, single, half-round obstacles at selected speeds. Only one obstacle was traversed during each run, and the speed was held constant. The obstacle was assumed to be rigid and fixed to a smooth, level, firm surface. The impact forces transmitted through the tire and suspension system were used to compute vertical displacements and vertical

accelerations at the vehicle center of gravity. Vertical and pitch displacements and accelerations at the center of gravity and the distance from the center of gravity to the driver were used to calculate the displacements and accelerations at the driver's seat. Roll motion was not a significant factor, since both front wheels of the vehicle contacted the obstacle at the same time.

34. The data predicted by these simulations (table 3) were used to develop peak vertical acceleration-obstacle height-impact speed relations. Predictions were also made for several obstacle heights not included in the test program to obtain a better definition of speed-obstacle height relations. For the XM410E1 truck, separate relations were developed for peak vertical acceleration at the driver's seat, the center of gravity, and the front axle. Similar relations were developed for the MEXA 10x10 test bed at the driver's seat and center of gravity. The acceleration and speed data in table 3 were plotted for each obstacle height, and the data points were connected by straight lines. From these relations, obstacle height-speed relations were developed for several levels of acceleration for both vehicles.

Peak vertical acceleration-speed relations

35. XM410E1. Peak vertical acceleration-speed relations for the XM410E1 truck at the driver's seat, center of gravity, and front axle are given in figs. a, b, and c, respectively, of plate 6 for 20-psi tire pressure. Separate curves are shown for obstacles of various heights. The open symbols represent obstacles (6, 8, 10, and 12 in.) for which measured data were available, and the closed symbols represent additional obstacles (7 and 9 in.) for which speed performance at 2.5-g accelerations were simulated.

36. The general trend of the relations presented in plate 6 are similar to those presented in plate 1 for the measured data in that the magnitude of peak vertical acceleration depends on location within the vehicle, obstacle height, and the speed at which the vehicle crosses the obstacle. For a given obstacle height and speed, the greatest accelerations occurred at the axles, followed by the driver's seat, and then

the center of gravity. The peak vertical acceleration at the driver's seat and the center of gravity varied in a seemingly erratic manner for the 9- and 10-in.-high obstacles. Such variations are attributable to the nonlinearities involved in the mathematical formulation of the dynamics prediction model.

37. MEXA 10x10. Peak vertical acceleration-speed relations for the MEXA 10x10 at the driver's seat and the center of gravity are given in figs. a and b, respectively, of plate 7. Separate curves are shown for the different obstacle heights. A 10-in.-high obstacle was used in addition to the 4-, 6-, and 8-in. obstacles used in the field tests to better define the relations.

38. The obvious trend is that acceleration increases with increases in speed and obstacle height, and the intensity of acceleration is noticeably greater at the driver's location. Unlike the measured data (plate 2), however, the predicted relations show no tendencies for the acceleration to level off and decrease beyond certain speeds. This is most likely due to the inability of this prediction model to realistically portray the effects of tire geometry and the tire-obstacle envelopment characteristics, which most certainly are responsible for this phenomenon. It is worth mentioning here that the tire compliance in the digital model representing the XM410E1 vehicle included both the tire geometry and tire-obstacle envelopment properties, and the results, as seen in plate 6, reflect this leveling or decreasing phenomenon.

Obstacle height-speed relations

39. Since a primary objective of the mathematical models is to adequately predict the limiting speed at which a vehicle can cross a given obstacle, the speeds and obstacle heights for selected values of acceleration that occurred at the driver's seat were read from the curves in plates 6a and 7a for the XM410E1 truck and MEXA 10x10 test bed, respectively. The data obtained in this manner are listed in the following tabulation.

| XM410E1 Truck, 20-psi Tire Pressure | | MEXA 10x10 Test Bed, 9-psi Tire Pressure | |
|---|---|---|---|
| Obstacle Height in. | Speed, mph | Obstacle Height in. | Speed, mph |
| | 2.5-g Acceleration | | |
| 6 | - | 4 | 13.5 |
| 7 | 11.5 | 6 | 8.0 |
| 8 | 11.0 | 8 | 6.5 |
| 9 | 4.4 | 10 | 5.0 |
| 10 | 3.5 | | |
| 11 | 2.5 | | |
| | 2.0-g Acceleration | | |
| 6 | - | 4 | 9.0 |
| 7 | 8.0 | 6 | 6.2 |
| 8 | 5.5 | 8 | 5.0 |
| 9 | 3.9 | 10 | 4.0 |
| 10 | 3.4 | | |
| 11 | 2.3 | | |
| | 1.5-g Acceleration | | |
| 6 | 7.8 | 4 | 6.0 |
| 7 | 5.0 | 6 | 4,5 |
| 8 | 4.2 | 8 | 3.7 |
| 9 | 3.0 | 10 | 3.0 |
| 10 | 3.0 | | |
| 11 | 2.1 | | |
| | 1.0-g Acceleration | | |
| 6 | 5.0 | 4 | 3.8 |
| 7 | - | 6 | 3.0 |
| 8 | 3.2 | 8 | 2.5 |
| 9 | 2.8 | 10 | 2.0 |
| 10 | 3.0 | | |
| 11 | 2.0 | | |

The above data are plotted in figs. a and b of plate 8 for the XM410E1 and MEXA 10x10, respectively; the curves were drawn on the basis of best visual fit. These figures show that for a given level of vertical acceleration, speed decreased as obstacle height increased.

## Comparison of Measured and Predicted Relations

40. A comparison of the measured and predicted relations of limiting speeds (i.e. the speeds at the occurrence of 2.5 g) versus obstacle height is shown in plate 9 for the two vehicles. The predicted values for the XM410E1 are consistently about 20 percent less than the measured values. However, the predicted values for the MEXA 10x10 are roughly about 15 percent greater than the measured values. Experience has shown that relations established from data measured in repeated field tests in which the quantity of interest is characterized by only a single point (such as the peak value) in the response-time history most often differs by a much larger percentage than those shown in plate 9. Consequently, it is felt that with the appropriate vehicle parameters as input, mathematical models such as described herein can be used to suitably simulate speed-obstacle height relations.

## PART IV: CONCLUSIONS AND RECOMMENDATIONS

### Conclusions

41. Based on the results reported herein, it is concluded that:

a. The magnitude of vertical acceleration depends on location in the vehicle, the height of the obstacle, and impact speed (paragraphs 21 and 24).

b. Vertical acceleration was consistently greatest at the front axle, smallest at the center of gravity, and intermediate at the driver's seat (paragraph 21).

c. Peak longitudinal acceleration tends to increase with obstacle height and speed (paragraphs 26 and 28).

d. The tolerance level established for longitudinal accelerations was never reached in the tests reported herein (paragraph 26) because the tests were stopped to avoid structural damage to the vehicle and bodily injury to the driver due to excessive vertical accelerations.

e. Tire pressure can significantly affect the peak acceleration response, with lower pressure producing smaller accelerations (paragraph 32).

f. For a given level of vertical acceleration, speed decreased with an increase in obstacle height (paragraph 39).

g. With the appropriate inputs, mathematical models can be used to simulate speed-obstacle height relations (paragraph 40).

### Recommendations

42. It is recommended that:

a. Additional data be obtained for a variety of vehicle types to better establish limiting speed-obstacle height relations and to determine if peak vertical accelerations and obstacle heights are suitable quantities for defining obstacle-crossing capabilities.

b. Further testing be conducted to determine the effects of various obstacle height-to-width ratios on dynamic response of vehicles.

c. Tests be conducted on a series of concave obstacles (ditches) of varying dimensions to provide experimental data for verification of vehicle dynamic response mathematical models.

d. A program be implemented to elucidate the effects of obstacle deformation on vehicle dynamic response. This program should be oriented toward studying the energy-absorbing capacity of soil obstacles of varying strengths. An important aspect of this program should be a search for parameters that adequately describe the damping characteristics of soil and for instruments that reliably measure those parameters, to provide a valid basis for the development of mathematical models for predicting dynamic response of vehicles crossing deformable obstacles.

## LITERATURE CITED


1. U. S. Army Engineer Waterways Experiment Station, CE, "An Analytical Model for Predicting Cross-Country Vehicle Performance; Application of Analytical Model to United States and Thailand Terrains," Technical Report No. 3-783, Appendix G (in preparation), Vicksburg, Miss.

2. Decell, J. L, "Mobility Exercise A Field Test Program; Performance of Selected MEXA and Military Vehicles in Selected Natural Terrains," Technical Report No. M-70-11, Report 5 (in preparation), U. S. Army Engineer Waterways Experiment Station, CE, Vicksburg, Miss.

3. Cardwell, D., "The Acceleration of Military Vehicles During Cross-Country Operations," Proceedings of a Symposium on Vehicle Ride held at the Advanced School of Automotive Engineering, Cranfield, New York, July 1963, edited by G. H. Tidbury (Cranfield International Symposium Series - Volume 4), MacMillan, New York, 1963, pp 3-36.

4. FMC Corporation, "A Computer Analysis of Vehicle Dynamics While Traversing Hard Surface Terrain Profiles," Contract Report No. 3-155, Feb 1966, U. S. Army Engineer Waterways Experiment Station, CE, Vicksburg, Miss.

5. Lessem, A. A., "Dynamics of Wheeled Vehicles, Mathematical Model for Traversal of Rigid Obstacles by a Pneumatic Tire," Technical Report No. M-68-1, Report 1, May 1968, U. S. Army Engineer Waterways Experiment Station, CE, Vicksburg, Miss.

Table 1

Vehicle Data

| | XM410E1 | MEXA 10x10 |
|---|---|---|
| Gross weight, lb | | |
| Empty, lb | 11,504 | 13,030 |
| Payload, lb | 5,000 | 5,000 |
| Test, lb | 16,505 | 18,030 |
| Wheel and tire data | | |
| Size* | 14x18 | 42x40-16A |
| Nominal width, in. | 14 | 40 |
| Rim diameter, in. | 18 | 16 |
| Wheel diameter, in. | 40 | 42 |
| Number of wheels | 8 | 10 |
| Number of axles | 4 | 5 |
| Average inflation pressure, psi | 12.2 | 7.3 |
| Average deflection, percent | 25 | 20 |
| Total contact area, sq in. | 975 | 2654 |
| Average contact pressure, psi | 16.9 | 6.8 |
| Ply rating | 6 | 4 |
| Ground clearance | | |
| Axle differential, in. | 15.0 | 11.5 |
| Interior | 20.0** | 26.0† |

* From manufacturer's specifications.
** Between 2d and 3d axles.
† Between front and rear units.

Table 2

Measured Test Data

| Item No. | Tire Inflation Pressure psi | Obstacle Height in. | Impact Speed mph | Peak Vertical Acceleration at Driver's Seat, g's | Peak Vertical Acceleration at Center of Gravity, g's | Peak Vertical Acceleration at Front Axle g's | Peak Longitudinal Acceleration at Center of Gravity, g's |
|---|---|---|---|---|---|---|---|
| | | | XM410E1, 8x8, 2-1/2-Ton Cargo Truck | | | | |
| 1 | 20* | 6 | 2.90 | 0.45 | 0.20 | 2.00 | -- |
| 2 | 20 | 6 | 5.35 | 1.45 | 0.55 | 4.20 | -- |
| 3 | 20 | 6 | 6.05 | 1.25 | 0.80 | 9.30 | 0.37 |
| 4 | 20 | 6 | 5.10 | 1.05 | 0.42 | 3.00 | 0.73 |
| 5 | 20 | 6 | 9.25 | 1.80 | 0.63 | 8.60 | 0.75 |
| 6 | 10-15** | 6 | 2.80 | 0.35 | 0.15 | 1.00 | 0.16 |
| 7 | 10-15 | 6 | 3.40 | 0.70 | 0.23 | 1.75 | 0.25 |
| 8 | 10-15 | 6 | 5.35 | 0.80 | 0.30 | 3.50 | 0.15 |
| 9 | 10-15 | 6 | 6.50 | 0.92 | 0.38 | 5.10 | 0.20 |
| 10 | 10-15 | 6 | 9.05 | 0.71 | 0.38 | 6.20 | 0.23 |
| 11 | 10-15 | 8 | 2.25 | 0.32 | 0.17 | 1.00 | 0.23 |
| 12 | 10-15 | 8 | 3.60 | 0.60 | 0.30 | 1.75 | 0.32 |
| 13 | 10-15 | 8 | 5.00 | 1.50 | 0.70 | 4.60 | 0.33 |
| 14 | 10-15 | 8 | 6.90 | 2.00 | 0.65 | 8.40 | 0.30 |
| 15 | 10-15 | 8 | 8.75 | 1.50 | 0.80 | 9.85 | 0.28 |
| 16 | 20 | 8 | 2.60 | 0.38 | 0.18 | 1.50 | 0.27 |
| 17 | 20 | 8 | 3.50 | 0.75 | 0.33 | 3.00 | 0.33 |
| 18 | 20 | 8 | 5.15 | 1.40 | 0.85 | 2.65 | 0.33 |
| 19 | 20 | 8 | 6.35 | 2.15 | 1.10 | 6.85 | 0.30 |
| 20 | 20 | 8 | 9.20 | 2.40 | 2.28 | 12.85 | 0.35 |
| 21 | 20 | 10 | 2.30 | 0.80 | 0.35 | 2.45 | 0.45 |
| 22 | 20 | 10 | 3.90 | 2.10 | 1.68 | 4.50 | 0.50 |
| 23 | 20 | 10 | 5.50 | 3.05 | 2.40 | 7.30 | 0.70 |
| 24 | 10-15 | 10 | 2.35 | 0.55 | 0.30 | 1.85 | 0.35 |
| 25 | 10-15 | 10 | 3.95 | 1.80 | 1.70 | 2.70 | 0.95 |

(Continued)

* Average tire deflection is 16.2 percent.

** Tire deflection is 25 percent.

Table 2 (Concluded)

| Item No. | Tire Inflation Pressure psi | Obstacle Height in. | Impact Speed mph | Peak Vertical Acceleration at Driver's Seat, g's | Peak Vertical Acceleration at Center of Gravity, g's* | Peak Vertical Acceleration at Front Axle g's | Peak Longitudinal Acceleration at Center of Gravity, g's |
|---|---|---|---|---|---|---|---|
| | | | XM410E1, 8x8, 2-1/2-Ton Cargo Truck (Continued) | | | | |
| 26 | 20 | 12 | 2.50 | 0.69 | .60 | 2.75 | 0.46 |
| 27 | 20 | 12 | 3.85 | 2.90 | 1.70 | 3.70 | 1.50 |
| | | | MEXA 10x10 Two-Unit Articulated Test Bed | | | | |
| 28 | 9** | 4 | 5.80 | 1.20 | 0.73 | -- | 0.28 |
| 29 | 9 | 4 | 12.20 | 1.75 | 1.65 | -- | 0.65 |
| 30 | 9 | 4 | 16.75 | 2.00 | 2.05 | -- | 0.79 |
| 31 | 9 | 4 | 21.75 | 2.08 | 1.25 | -- | 0.90 |
| 32 | 9 | 6 | 3.00 | 0.65 | 0.35 | -- | 0.25 |
| 33 | 9 | 6 | 2.90 | 0.50 | 0.25 | -- | 0.18 |
| 34 | 9 | 6 | 3.85 | 1.25 | 0.60 | -- | 0.25 |
| 35 | 9 | 6 | 3.55 | 1.20 | 0.65 | -- | 0.25 |
| 36 | 9 | 6 | 5.00 | 1.95 | 1.10 | -- | 1.37 |
| 37 | 9 | 6 | 5.00 | 1.65 | .95 | -- | 1.60 |
| 38 | 9 | 6 | 8.20 | 3.10 | 1.95 | -- | 1.25 |
| 39 | 9 | 6 | 8.00 | 2.50 | 1.75 | -- | 1.10 |
| 40 | 9 | 6 | 8.90 | 3.10 | 1.50 | -- | 1 05 |
| 41 | 9 | 6 | 9.50 | 4.35 | 3.50 | -- | 1.06 |
| 42 | 9 | 6 | 12.55 | 2.70 | 1.75 | -- | 0.85 |
| 43 | 9 | 6 | 13.90 | 3.50 | 2.35 | -- | 1.60 |
| 44 | 9 | 6 | 16.20 | 3.65 | 2.75 | -- | 1.80 |
| 45 | 9 | 6 | 15.60 | 3.50 | 2.65 | -- | 1.78 |
| 46 | 9 | 6 | 17.00 | 3.45 | 2.75 | -- | 1.85 |
| 47 | 9 | 6 | 19.10 | 3.30 | 2.95 | -- | 1.73 |
| 48 | 9 | 8 | 3.50 | 0.90 | 0.65 | -- | 0.26 |
| 49 | 9 | 8 | 4.90 | 1.90 | 1.48 | -- | 0.93 |
| 50 | 9 | 8 | 7.15 | 2.35 | 2.40 | -- | 0.80 |

* Front unit.

** Average deflection is 16.9 percent.

Table 3

Predicted Data

| Run No. | Obstacle Height in. | Impact Speed mph | Peak Vertical Acceleration at Driver's Seat g's | Peak Vertical Acceleration at Center of Gravity g's | Peak Vertical Acceleration at Front Axle g's |
|---|---|---|---|---|---|
| | | XM410E1, 8x8, 2-1/2-ton Cargo Truck* | | | |
| 1 | 4 | 3 | 0.43 | 0.21 | 1.07 |
| 2 | 4 | 5 | 0.68 | 0.32 | 1.31 |
| 3 | 4 | 7 | 0.70 | 0.48 | 2.13 |
| 4 | 4 | 9 | 0.78 | 0.46 | 3.25 |
| 5 | 4 | 12 | 0.80 | 0.48 | 4.63 |
| 6 | 4 | 15 | 0.79 | 0.49 | 6.65 |
| 7 | 4 | 20 | 0.76 | 0.42 | 7.29 |
| 8 | 6 | 3 | 0.69 | 0.33 | 1.77 |
| 9 | 6 | 5 | 1.00 | 0.54 | 2.65 |
| 10 | 6 | 7 | 1.32 | 0.79 | 4.71 |
| 11 | 6 | 9 | 1.73 | 1.17 | 5.66 |
| 12 | 6 | 12 | 1.80 | 1.43 | 8.36 |
| 13 | 6 | 15 | 2.06 | 1.24 | 12.68 |
| 14 | 6 | 18 | 1.85 | 1.36 | 16.00 |
| 15 | 6 | 20 | 2.45 | 1.18 | 18.79 |
| 16 | 7 | 5 | 1.50 | 0.76 | 3.48 |
| 17 | 7 | 7 | 1.94 | 1.27 | 4.95 |
| 18 | 7 | 10 | 2.19 | 1.80 | 11.36 |
| 19 | 7 | 12 | 2.62 | 1.67 | 14.71 |
| 20 | 7 | 15 | 2.99 | 1.74 | 17.94 |
| 21 | 7 | 17 | 2.70 | 1.97 | 19.36 |
| 22 | 7 | 20 | 3.34 | 1.86 | 22.83 |
| 23 | 8 | 3 | 0.87 | 0.52 | 1.65 |
| 24 | 8 | 5 | 1.90 | 0.97 | 3.87 |
| 25 | 8 | 7 | 2.12 | 1.67 | 5.66 |
| 26 | 8 | 9 | 2.29 | 1.88 | 11.17 |
| 27 | 8 | 12 | 3.10 | 1.52 | 16.38 |
| 28 | 9 | 3 | 1.20 | 0.73 | 2.34 |
| 29 | 9 | 5 | 2.95 | 1.59 | 5.74 |
| 30 | 9 | 6 | 2.54 | 2.15 | 6.69 |
| 31 | 10 | 3 | 1.81 | 1.09 | 3.50 |
| 32 | 10 | 4 | 3.66 | 2.50 | -- |
| 33 | 10 | 5 | 3.10 | 2.17 | 7.21 |
| 34 | 10 | 5.5 | 3.21 | 2.35 | 7.10 |
| 35 | 10 | 6 | 2.62 | 1.95 | 7.23 |

(Continued)

* Average tire deflection 18.2 percent; 20-psi tire pressure.

Table 3 (Concluded)

| Run No. | Obstacle Height in. | Impact Speed mph | Peak Vertical Acceleration at Driver's Seat g's | Peak Vertical Acceleration at Center of Gravity g's | Peak Vertical Acceleration at Front Axle g's |
|---|---|---|---|---|---|
| | | XM410E1, 8x8, 2-1/2-ton Cargo Truck (Continued) | | | |
| 36 | 12 | 2 | 0.76 | 0.41 | 2.84 |
| 37 | 12 | 3 | 3.06 | 1.54 | 6.71 |
| 38 | 12 | 5 | 3.85 | 3.01 | 7.45 |
| 39 | 12 | 8 | 3.98 | 2.08 | 12.14 |
| | | MEXA 10x10 Two-Unit Articulated Test Bed* | | | |
| 1 | 4 | 5 | 1.35 | 1.00** | - |
| 2 | 4 | 10 | 2.15 | 1.25 | - |
| 3 | 4 | 15 | 2.62 | 1.65 | - |
| 4 | 4 | 20 | 2.95 | 1.85 | - |
| 5 | 6 | 5 | 1.70 | 1.35 | - |
| 6 | 6 | 10 | 2.95 | 1.80 | - |
| 7 | 6 | 15 | 3.85 | 2.40 | - |
| 8 | 6 | 20 | 4.70 | 2.70 | - |
| 9 | 8 | 5 | 2.00 | 1.70 | - |
| 10 | 8 | 10 | 3.70 | 2.35 | - |
| 11 | 8 | 15 | 4.50 | 2.95 | - |
| 12 | 8 | 20 | 5.30 | 3.45 | - |
| 13 | 10 | 5 | 2.45 | 2.10 | - |
| 14 | 10 | 10 | 4.45 | 2.65 | - |
| 15 | 10 | 15 | 5.45 | 3.52 | - |

* Tire inflation pressure, 9 psi.
** Front unit.

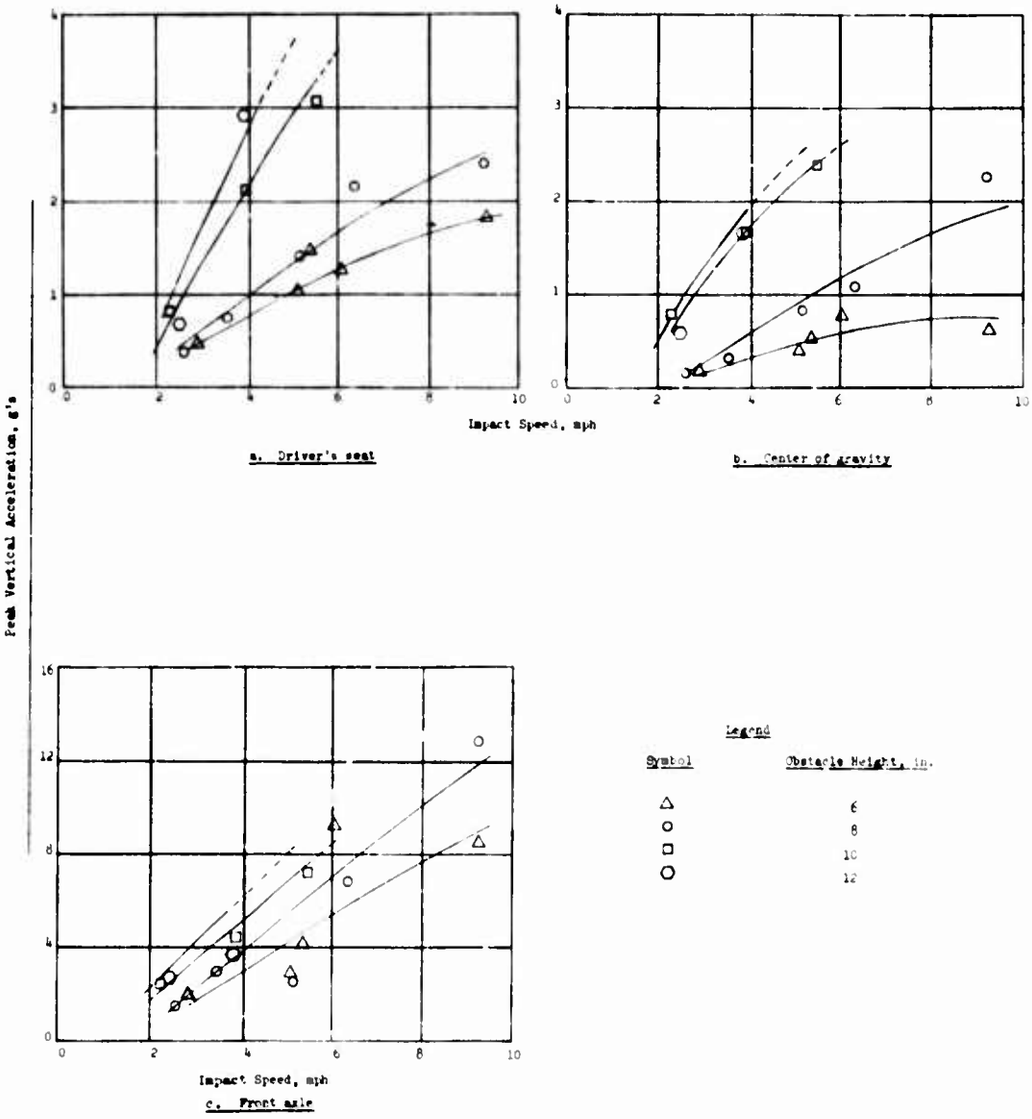


PEAK VERTICAL ACCELERATION-IMPACT SPEED RELATIONS FOR SELECTED OBSTACLE HEIGHTS AND VEHICLE POSITIONS (XM410E1, MEASURED DATA, 20-PSI TIRE PRESSURE)

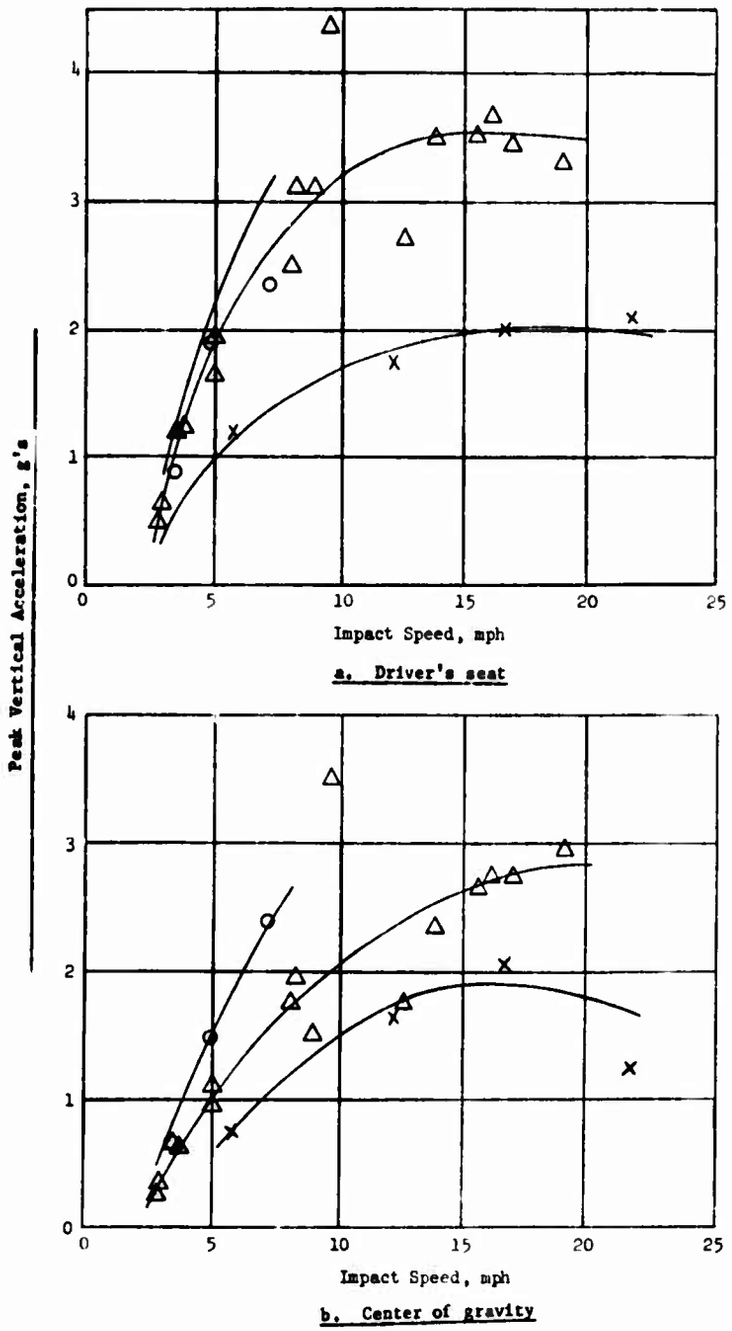


| Legend | |
|---|---|
| Symbol | Obstacle Height, in. |
| × | 4 |
| △ | 6 |
| ○ | 8 |

PEAK VERTICAL ACCELERATION-IMPACT SPEED RELATIONS FOR SELECTED OBSTACLE HEIGHTS AND VEHICLE POSITIONS (MEXA 10x10, MEASURED DATA, 9-PSI TIRE PRESSURE)

PLATE 2

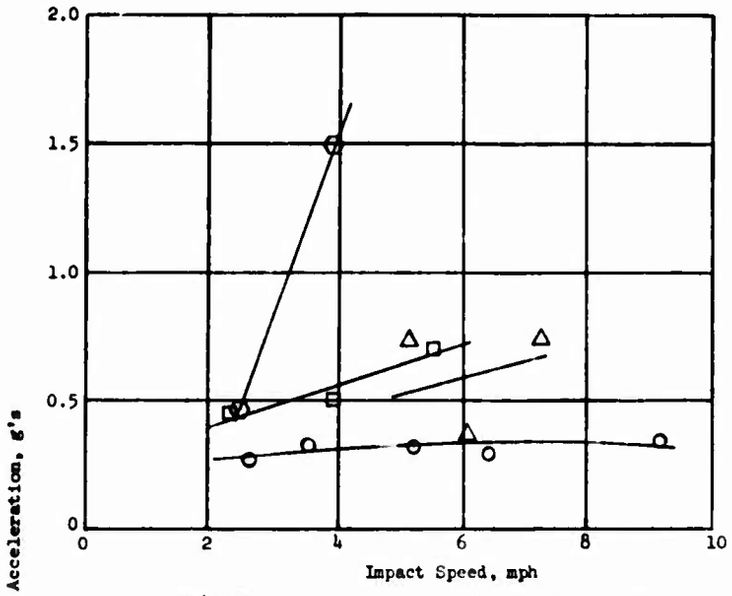


a. XM410E1 center of gravity, 20-psi tire pressure

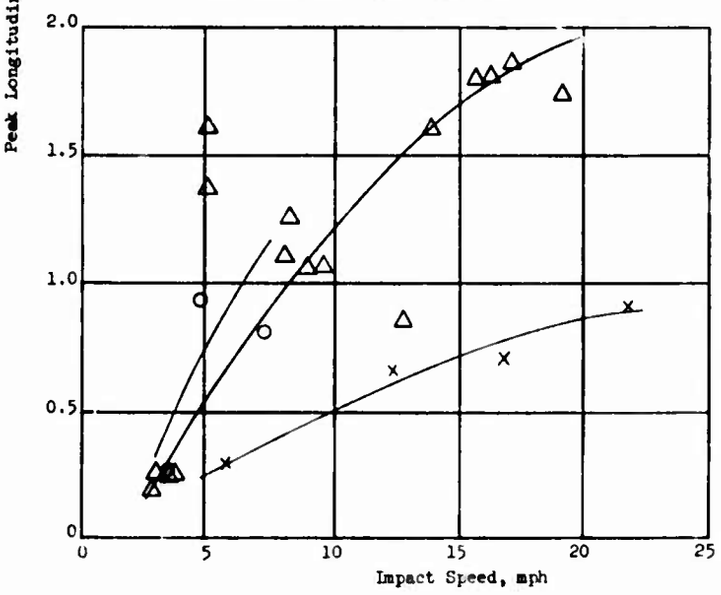


b MEXA 10x10, center of gravity, 9-psi tire pressure

| Legend | |
|---|---|
| Symbol | Obstacle Height, in. |
| ✕ | 4 |
| △ | 6 |
| ○ | 8 |
| □ | 10 |
| ⬡ | 12 |

PEAK LONGITUDINAL ACCELERATION-IMPACT SPEED RELATIONS FOR SELECTED OBSTACLE HEIGHTS (MEASURED DATA)



PLATE 3

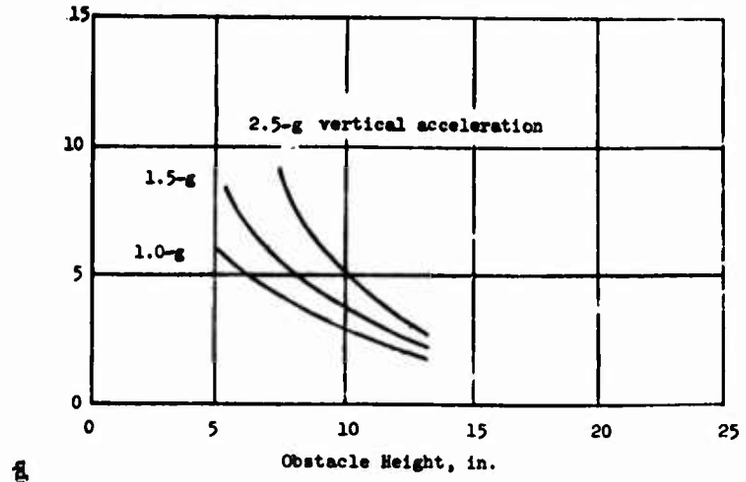


a. XM410E1 Truck

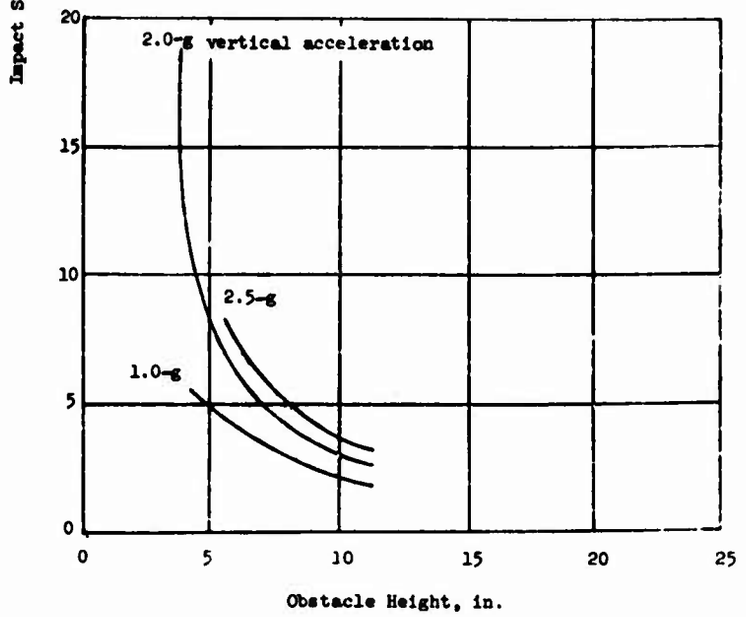


b. MEXA 10x10 Test Bed

SPEED-OBSTACLE HEIGHT RELATIONS
AT DRIVER'S SEAT (MEASURED DATA)

PLATE 4

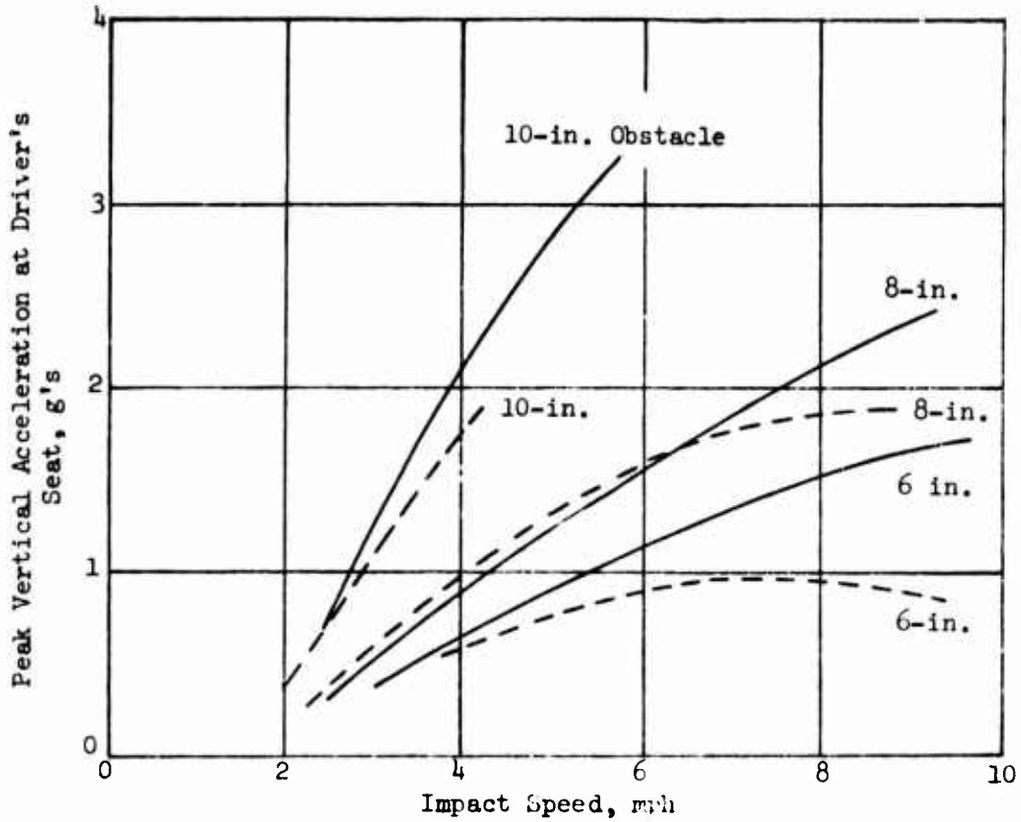


Legend

——— 20-psi tire pressure, 18.2 percent average tire deflection

----- 10- to 15-psi tire pressure, 25 percent average tire deflection

PEAK VERTICAL ACCELERATION-IMPACT SPEED RELATIONS FOR SELECTED OBSTACLE HEIGHTS AND TIRE PRESSURES (XM410E1, MEASURED DATA)

PLATE 5

PLATE 6

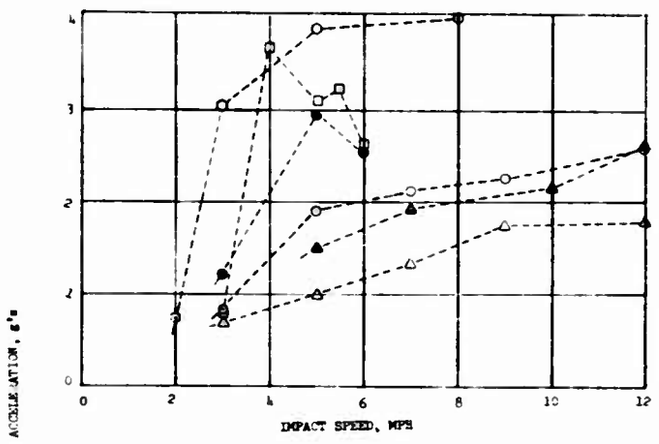


a. Driver's Seat

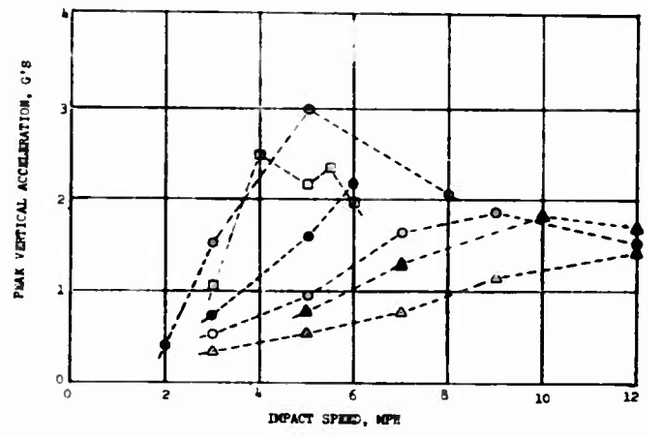


b. Center of Gravity

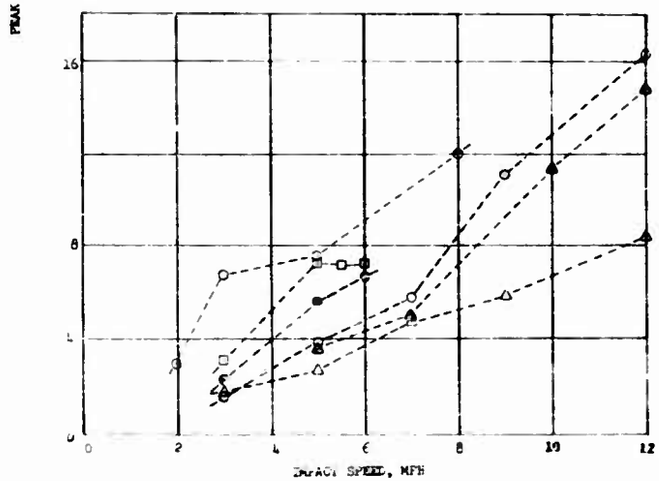


c. Front Axle

Legend

| Symbol | Obstacle Height, in. |
|---|---|
| △ | 6 |
| ▲ | 7 |
| ○ | 8 |
| ◕ | 9 |
| □ | 10 |
| ○ | 12 |

PEAK VERTICAL ACCELERATION-IMPACT SPEED RELATIONS FOR SELECTED OBSTACLE HEIGHTS AND VEHICLE POSITIONS (XM410E1, PREDICTED DATA, 20-PSI TIRE PRESSURE)

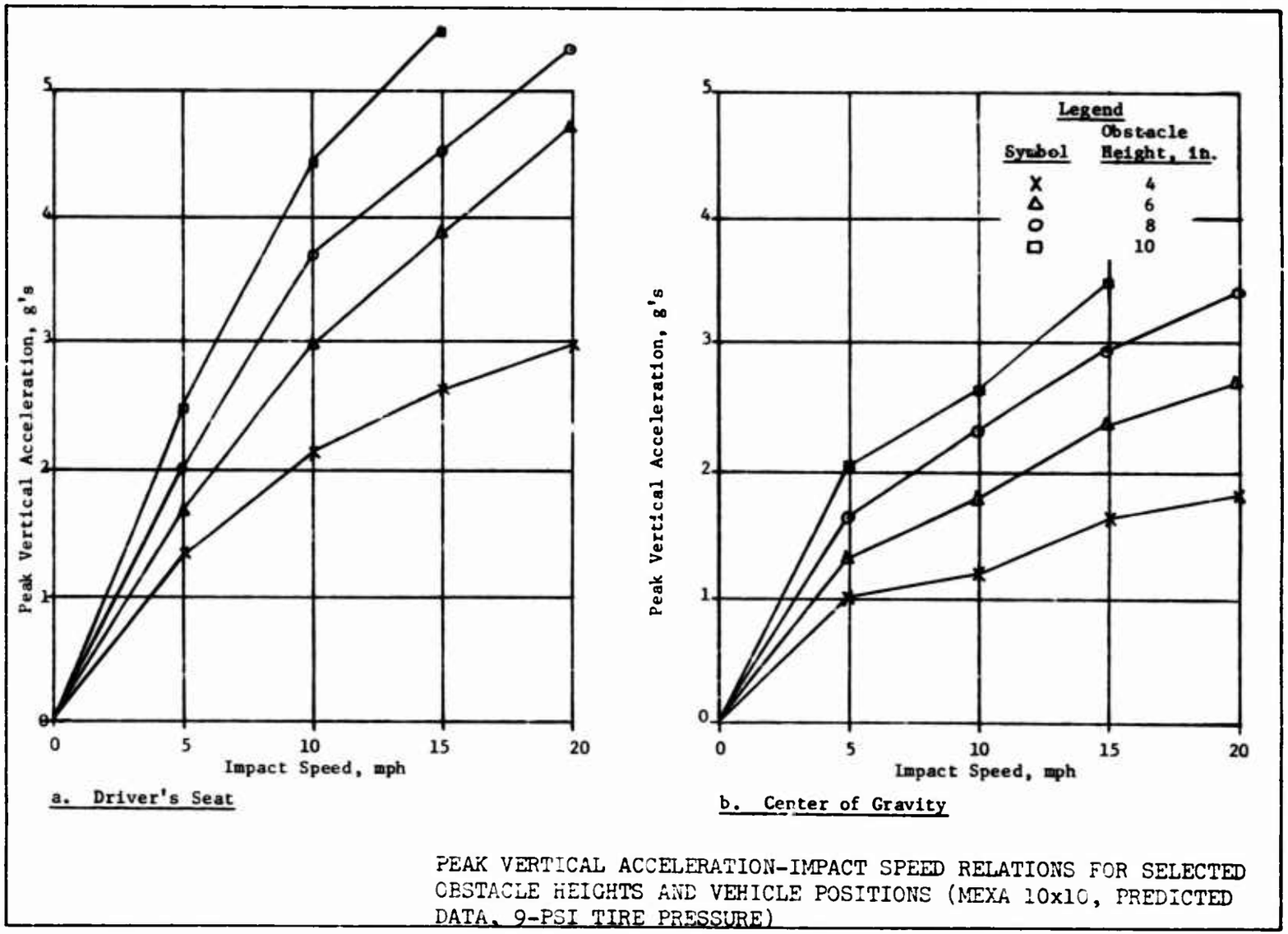


PEAK VERTICAL ACCELERATION-IMPACT SPEED RELATIONS FOR SELECTED OBSTACLE HEIGHTS AND VEHICLE POSITIONS (MEXA 10x10, PREDICTED DATA, 9-PSI TIRE PRESSURE)

PLATE 7

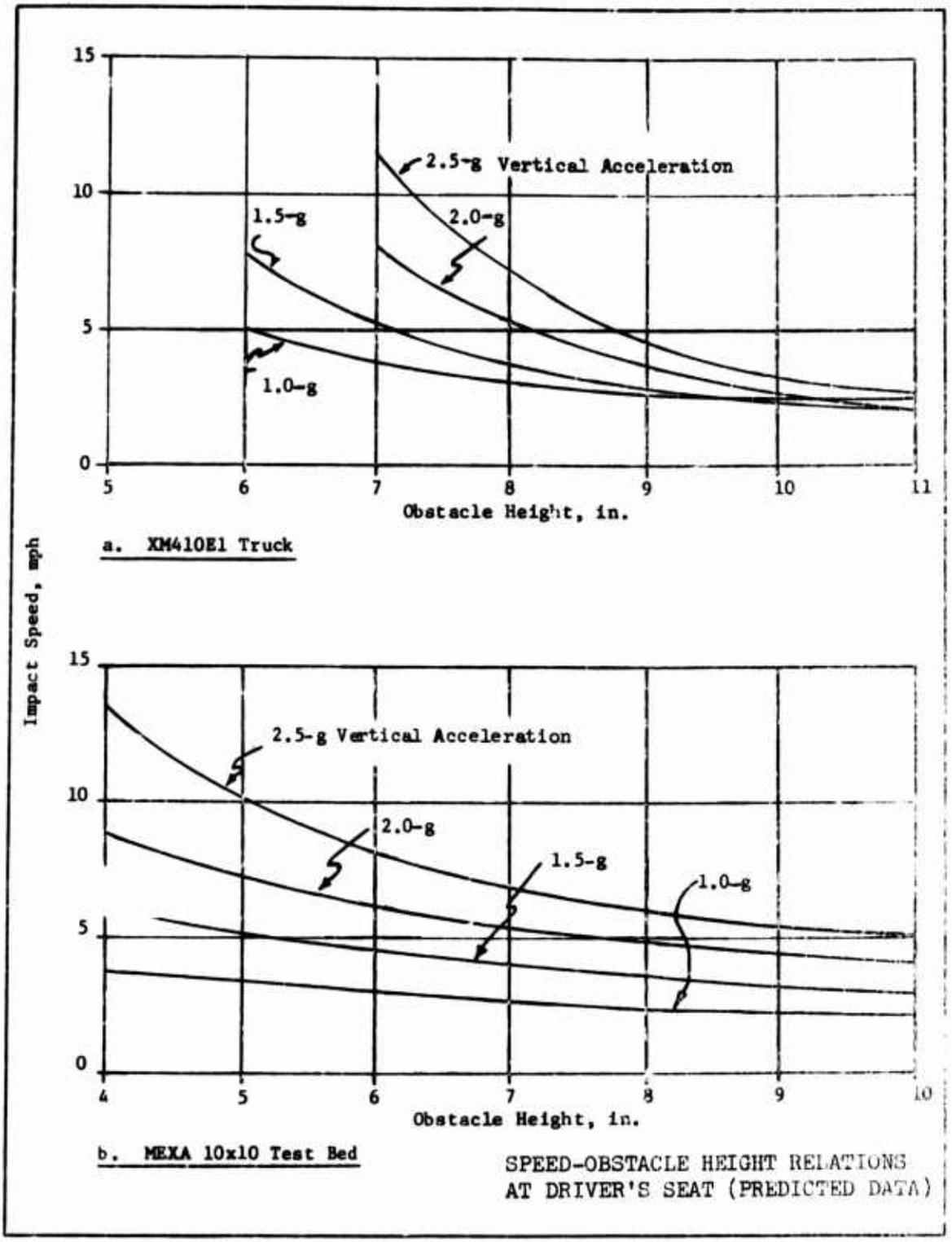


SPEED-OBSTACLE HEIGHT RELATIONS
AT DRIVER'S SEAT (PREDICTED DATA)

PLATE 8

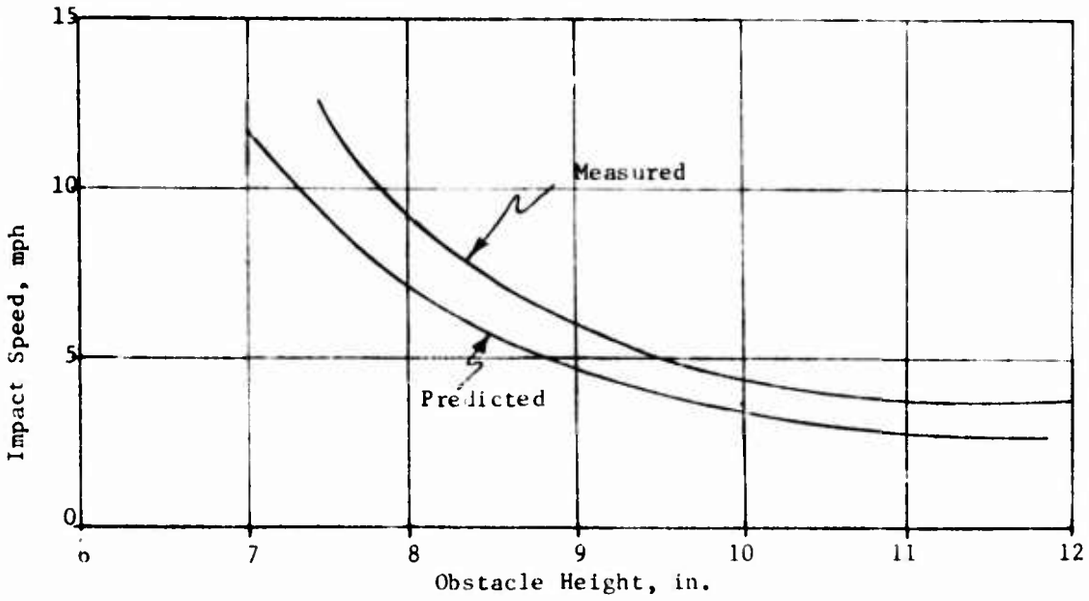


a. XM410E1 Truck

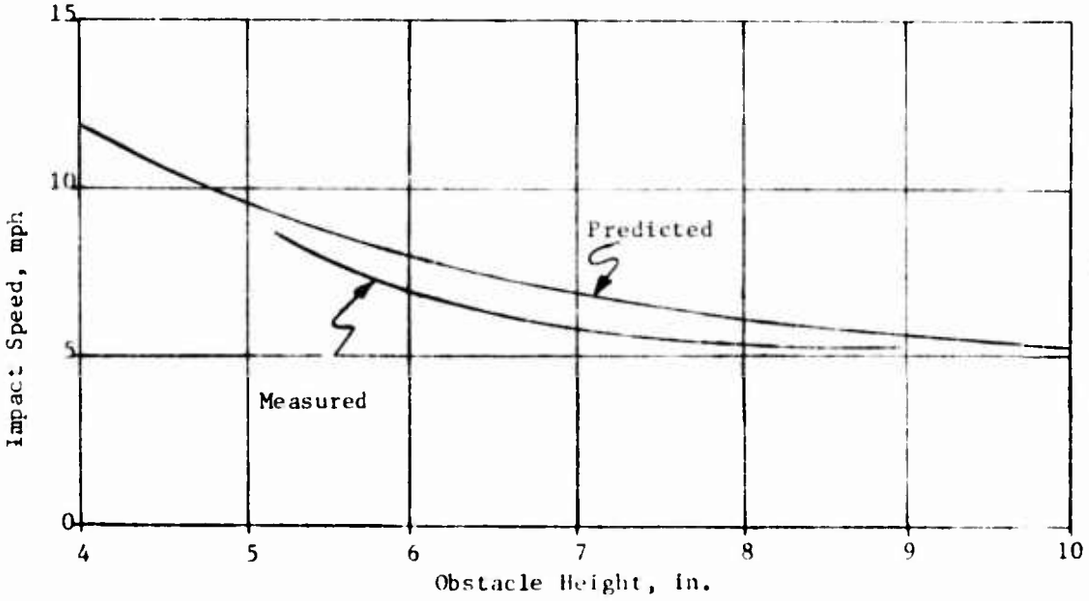


b. MEXA 10x10 Test Bed

COMPARISON OF MEASURED AND PREDICTED SPEED-OBSTACLE HEIGHT RELATIONSHIPS FOR 2.5-g VERTICAL ACCELERATION

## APPENDIX A: MATHEMATICAL MODELS FOR PREDICTING VEHICLE DYNAMIC RESPONSE

### Simulation of MEXA 10x10

1. A simplified set of equations was developed to describe the dynamic aspects of the 10x10 MEXA (articulated) test bed. These equations are complete in that they portray the pertinent translational and rotational motions of each unit. A schematic of the vehicle system is shown in fig. A1. An energy approach (Lagrangian) was used to formulate the equations of motion. This approach automatically eliminates forces of constraint (force on the hitch point in this case) that present formidable difficulties when conventional methods are used.

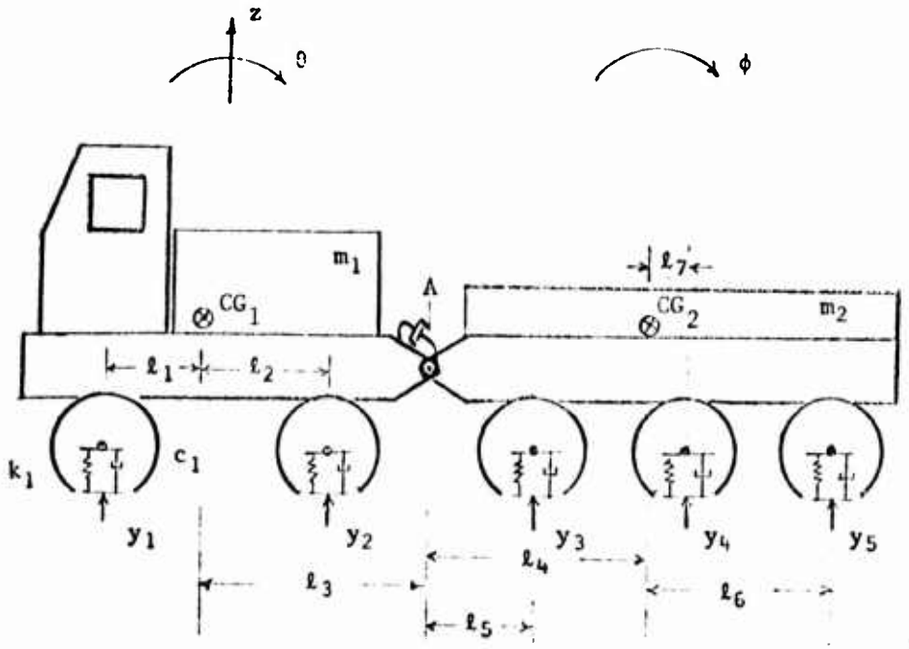


Fig. A1. Schematic of MEXA 10x10 test bed

2. The movements of the front unit will be a vertical motion (z) of the center of gravity (CG) and a pitching ($\theta$) about the center of gravity (CG). The rear unit motions are those of the hitch point (A) together with a pitching motion ($\phi$) about the rear unit center of gravity (CG). (This constraint eliminates the explicit formulation of rear unit bounce. The vertical displacement of the high point A is $z - \ell_3\theta$. The vertical displacement of the rear unit $CG_2$ is $z - \ell_3\theta - \ell_4\theta$. The y-coordinates represent the terrain or obstacle inputs to the system.

3. The coordinates $z$, $\theta$, and $\phi$ describe completely the bounce and pitch motions of the two units. Lagrange's equation was used to derive the equations of motion, since this approach reduces the conventional vector equations to scalar forms by use of energy concepts, and affords the simplest, most straightforward approach for systems of this type.

4. The Lagrange equation is

$$\frac{d}{dt}\left[\frac{\partial T}{\partial \dot{q}_i}\right] - \frac{\partial T}{\partial q_i} + \frac{\partial V}{\partial q_i} + \frac{\partial D}{\partial \dot{q}_i} = Q_i \qquad (1)$$

where

$T$ = kinetic energy of the system

$V$ = potential energy of the system

$D$ = damping energy of the system

$q$ = any generalized coordinates, in this case $q_1 = z$, $q_2 = \theta$, and $q_3 = \phi$

$Q_i$ = any externally applied forces, i.e. all those that supply energy to the system

5. By using the small-angle assumption, the following energy equations can be developed:

a. Kinetic energy of the system =

$$T = \frac{1}{2} m_1 \dot{z}^2 + \frac{1}{2} I_1 \dot{\theta}^2 + \frac{1}{2} m_2 (\dot{z} - \ell_3 \dot{\theta} - \ell_4 \dot{\phi})^2 + \frac{1}{2} I_2 \dot{\phi}^2$$

b. Potential energy of the system =

$$V = \frac{1}{2} K_1 (z + \ell_1 \theta - y_i)^2 + \frac{1}{2} K_2 (z - \ell_2 \theta - y_2)^2 + \frac{1}{2} K_3 (z - \ell_3 \theta - \ell_5 \phi - y_3)^2$$
$$+ \frac{1}{2} K_4 [z - \ell_3 \theta - (\ell_4 + \ell_7)\phi - y_4]^2 + \frac{1}{2} K_5 [z - \ell_3 \theta - (\ell_4 + \ell_6)\phi - y_5]^2$$
$$+ m_1 g z + m_2 g (z - \ell_3 \theta - \ell_4 \phi)$$

c. Damping energy of the system =

$$D = \frac{1}{2} C_1 (\dot{z} + \ell_1 \dot{\theta} - \dot{y}_i)^2 + \frac{1}{2} C_2 (\dot{z} - \ell_2 \dot{\theta} - \dot{y}_2)^2 + \frac{1}{2} C_3 (\dot{z} - \ell_3 \dot{\theta} - \ell_5 \dot{\phi} - \dot{y}_3)^2$$
$$+ \frac{1}{2} C_4 [\dot{z} - \ell_3 \dot{\theta} - (\ell_4 + \ell_7)\dot{\phi} - \dot{y}_4]^2 + \frac{1}{2} C_5 [\dot{z} - \ell_3 \dot{\theta} - (\ell_4 + \ell_6)\dot{\phi} - \dot{y}_5]^2$$

6. Using each of the three coordinates, one at a time, and performing the operations on the energy equations above as specified by equation 1, beginning with the z coordinate, yields:

$$\frac{\partial T}{\partial \dot{z}} = m_1 \dot{z} + m_2 (\dot{z} - \ell_3 \dot{\theta} - \ell_4 \dot{\phi}) \quad \therefore \frac{d}{dt}\left(\frac{\partial T}{\partial \dot{z}}\right) = m_1 \ddot{z} + m_2 \ddot{z} - m_2 \ell_3 \ddot{\theta} - m_2 \ell_4 \ddot{\phi}$$

$$\frac{\partial T}{\partial z} = 0$$

$$\frac{\partial V}{\partial z} = k_1 (z + \ell_1 \theta - y_1) + k_2 (z - \ell_2 \theta - y_2) + k_3 (z - \ell_3 \theta - \ell_5 \phi - y_3)$$
$$+ k_4 [z - \ell_3 \theta - (\ell_4 + \ell_7)\phi - y_4] + k_5 [z - \ell_3 \theta - (\ell_4 + \ell_6)\phi - y_5]$$
$$+ (m_1 + m_2) g$$

$$\frac{\partial D}{\partial \dot{z}} = C_1 (\dot{z} + \ell_1 \dot{\theta} - \dot{y}_1) + C_2 (\dot{z} - \ell_2 \dot{\theta} - \dot{y}_2) + C_3 (\dot{z} - \ell_3 \dot{\theta} - \ell_5 \dot{\phi} - \dot{y}_3)$$
$$+ C_4 [\dot{z} - \ell_3 \dot{\theta} - (\ell_4 + \ell_7)\dot{\phi} - \dot{y}_4] + C_5 [\dot{z} - \ell_3 \dot{\theta} - (\ell_4 + \ell_6)\dot{\phi} - \dot{y}_5]$$

7. Substituting the results of these derivatives into equation 1 yields the first equation of motion, which is the vertical motion of the center of gravity of the front unit. Note: $Q_1 = 0$ for this system because there are no externally applied forces. The forcing functions $y_1, y_2 \ldots, y_5$ are displacements and are accounted for in the energy expressions.

$$(m_1 + m_2)\ddot{z} - m_2\ell_3\ddot{\theta} - m_2\ell_4\ddot{\phi} + k_1(z + \ell_1\theta - y_1) + k_2(z - \ell_2\theta - y_2) \tag{2}$$

$$+ k_3(z - \ell_3\theta - \ell_5\phi - y_3) + k_4[z - \ell_3\theta - (\ell_4 + \ell_7)\phi - y_4]$$

$$+ k_5[z - \ell_3\theta - (\ell_4 + \ell_6)\phi - y_5] + (m_1 + m_2)g + C_1(\dot{z} + \ell_1\dot{\theta} - \dot{y}_1) + C_2(\dot{z} - \ell_2\dot{\theta} - \dot{y}_2)$$

$$+ C_3(\dot{z} - \ell_3\dot{\theta} - \ell_5\dot{\phi} - \dot{y}_3) + C_4[\dot{z} - \ell_3\dot{\theta} - (\ell_4 + \ell_7)\dot{\phi} - y_4]$$

$$+ C_5[\dot{z} - \ell_3\dot{\theta} - (\ell_4 + \ell_6)\dot{\phi} - \dot{y}_5] = 0$$

Now considering the $\theta$ coordinate:

$$\frac{\partial T}{\partial \dot{\theta}} = I_1\dot{\theta} - m_2\ell_3(\dot{z} - \ell_3\dot{\theta} - \ell_4\dot{\phi})$$

$$\therefore \frac{d}{dt}\left(\frac{\partial T}{\partial \dot{\theta}}\right) = I_1\ddot{\theta} - m_2\ell_3\ddot{z} + m_2\ell_3^2\ddot{\theta} + m_2\ell_3\ell_4\ddot{\phi}$$

$$\frac{\partial T}{\partial \theta} = 0$$

$$\frac{\partial V}{\partial \theta} = k_1\ell_1(z + \ell_1\theta - y_1) - k_2\ell_2(z - \ell_2\theta - y_2) - k_3\ell_3(z - \ell_3\theta - \ell_5\phi - y_3)$$

$$- k_4\ell_3[z - \ell_3\theta - (\ell_4 + \ell_7)\phi - y_4] - k_5\ell_3[z - \ell_3\theta - (\ell_4 + \ell_6)\phi - y_5]$$

$$- m_2g\ell_3$$

$$\frac{\partial D}{\partial \dot{\theta}} = C_1\ell_1(\dot{z} + \ell_1\dot{\theta} - \dot{y}_1) - C_2\ell_2(\dot{z} - \ell_2\dot{\theta} - \dot{y}_2) - C_3\ell_3(\dot{z} - \ell_3\dot{\theta} - \ell_5\dot{\phi} - \dot{y}_3)$$

$$- C_4\ell_3[\dot{z} - \ell_3\dot{\theta} - (\ell_4 + \ell_7)\dot{\phi} - \dot{y}_4] - C_5\ell_3[\dot{z} - \ell_3\dot{\theta} - (\ell_4 + \ell_6)\dot{\phi} - \dot{y}_5]$$

8. Substituting these results in equation 1 yields the pitch motion of the front unit about the center of gravity:

$$(I_1 + m_2\ell_3^2)\ddot{\theta} - m_2\ell_3\ddot{z} + m_2\ell_3\ell_4\ddot{\phi} + k_1\ell_1(z + \ell_1\theta - y_1) - k_2\ell_2(z - \ell_2\theta - y_2)$$

$$- k_3\ell_3(z - \ell_3\theta - \ell_5\phi - y_3) - k_4\ell_3[z - \ell_3\theta - (\ell_4 + \ell_7)\phi - y_4] \qquad (3)$$

$$- k_5\ell_3[z - \ell_3\theta - (\ell_4 + \ell_6)\phi - y_5] - m_2g\ell_3 + C_1\ell_1(\dot{z} + \ell_1\dot{\theta} - \dot{y}_1) - C_2\ell_2(\dot{z} - \ell_2\dot{\theta} - \dot{y}_2)$$

$$- C_3\ell_3(\dot{z} - \ell_3\dot{\theta} - \ell_5\dot{\phi} - \dot{y}_3) - C_4\ell_3[\dot{z} - \ell_3\dot{\theta} - (\ell_4 + \ell_7)\dot{\phi} - \dot{y}_4]$$

$$- C_5\ell_3[\dot{z} - \ell_3\dot{\theta} - (\ell_4 + \ell_6)\dot{\phi} - \dot{y}_5] + C_6\dot{\theta} = 0$$

Considering now the $\phi$ coordinate:

$$\frac{\partial T}{\partial \dot{\phi}} = I_2\dot{\phi} - m_2\ell_4(\dot{z} - \ell_3\dot{\theta} - \ell_4\dot{\phi}) \quad \therefore \frac{d}{dt}\left(\frac{\partial T}{\partial \dot{\phi}}\right) = I_2\ddot{\phi} - m_2\ell_4(\ddot{z} - \ell_3\ddot{\theta} - \ell_4\ddot{\phi})$$

$$\frac{\partial T}{\partial \phi} = 0$$

$$\frac{\partial V}{\partial \phi} = -k_3\ell_5(z - \ell_3\theta - \ell_5\phi - y_3) - k_4(\ell_4 + \ell_7)[z - \ell_3\theta - (\ell_4 + \ell_7)\phi - y_4]$$

$$- k_5(\ell_4 + \ell_6)[z - \ell_3\theta - (\ell_4 + \ell_6)\phi - y_5] - m_2g\ell_4$$

$$\frac{\partial D}{\partial \dot{\phi}} = -C_3\ell_5(\dot{z} - \ell_3\dot{\theta} - \ell_5\dot{\phi} - \dot{y}_3) - C_4(\ell_4 + \ell_7)[\dot{z} - \ell_3\dot{\theta} - (\ell_4 + \ell_7)\dot{\phi} - \dot{y}_4]$$

$$- C_5(\ell_4 + \ell_6)[\dot{z} - \ell_3\dot{\theta} - (\ell_4 + \ell_6)\dot{\phi} - \dot{y}_5]$$

9. Substituting into equation 1 results in the pitching motion of the rear unit about the center of gravity:

$$I_2\ddot{\phi} - m_2\ell_4\ddot{z} + m_2\ell_3\ell_4\ddot{\theta} + m_2\ell_4^2\ddot{\phi} - k_3\ell_5(z - \ell_3\theta - \ell_5\phi - y_3) - k_4(\ell_4 + \ell_7)$$

$$[z - \ell_3\theta - (\ell_4 + \ell_7)\phi - y_4] - k_5(\ell_4 + \ell_6)[z - \ell_3\theta - (\ell_4 + \ell_6)\phi - y_5]$$

$$- m_2g\ell_4 - C_3\ell_5(\dot{z} - \ell_3\dot{\theta} - \ell_5\dot{\phi} - \dot{y}_3) - C_4(\ell_4 + \ell_7)$$

$$[\dot{z} - \ell_3\dot{\theta} - (\ell_4 + \ell_7)\dot{\phi} - \dot{y}_4] - C_5(\ell_4 + \ell_6)\ [\dot{z} - \ell_3\dot{\theta} - (\ell_4 + \ell_6)\dot{\phi} \quad \dot{y}_5] + C_6\dot{\theta} = 0$$

10. The symbology used in the preceding equations together with the numerical values of the input parameters are as follows:

$\ddot{z}, \dot{z}, z$ = vertical motions of the center of gravity of the front unit, i.e. the acceleration, velocity, and displacement, respectively.

$\ddot{\theta}, \dot{\theta}, \theta$ = angular motions about the center of gravity of the front unit with reference to the horizontal plane, i.e. acceleration, velocity, and displacement, respectively.

$\ddot{\phi}, \dot{\phi}, \phi$ = angular motions about the center of gravity of the rear unit

$g$ = acceleration due to gravity = 386 in./sec$^2$.

$\ell_1$ = distance from $CG_1$ of front unit to front axle = 50 in.

$\ell_2$ = distance from $CG_1$ of front unit to rear axle of front unit = 27 in.

$\ell_3$ = distance from $CG_1$ of front unit to hitch point = 80.5 in.

$\ell_4$ = distance from $CG_2$ of rear unit to hitch point = 87.5 in.

$\ell_5$ = distance from leading axle of rear unit to hitch point = 36.5 in.

$\ell_6$ = distance from $CG_2$ of rear unit to rear axle of rear unit = 51 in.

$\ell_7$ = distance from $CG_2$ of rear unit to middle axle of rear unit = 9.6 in.

$y_1, y_2 \ldots y_5$ = terrain forcing functions.

$k_1, k_2 \ldots k_5$ = tire spring, determined from static load-deflection curves. See fig. A2 $\quad k_1 = k_2 = \ldots k_5$ .

$C_1, C_2 \ldots C_5$ = tire damping determined from the logarithmic decrement obtained from accelerometer outputs as a result of drop tests = 4.17 lb/in./sec .

$C_6$ = hitch point dampling = 5.71 lb/in./sec.

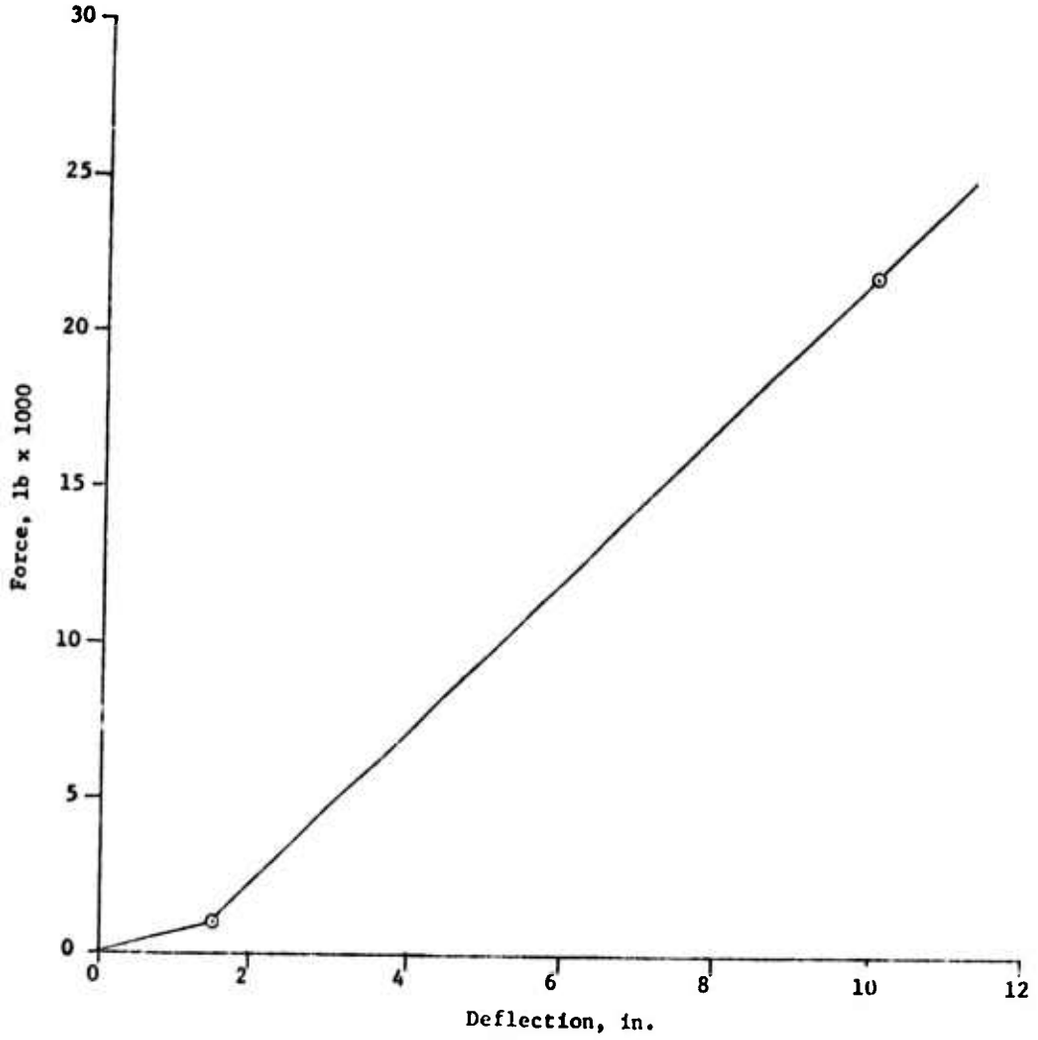


Fig. A2. Force-deflection relation for 42x40-16A, 4-PR tire at 9-psi inflation pressure, mounted on MEXA 10x10 test bed

$m_1$, $m_2$ = one half of the respective masses of the front and rear units = 10.2 and 13.0 lb-sec$^2$/in.

$I_1$, $I_2$ = one-half of the moments of inertia of front and rear units = 19,952 and 27,979 lb-sec-in.

11. To obtain the motions of the model at locations other than at the centers of gravity requires a combination of the appropriate translational and rotational motions. For example, the acceleration at the driver's seat was determined from the following equation:

$$\ddot{z}_D = \ddot{z} + \ell\ddot{\theta}$$

where $\ell$ = distance from the CG of the front unit to the driver's location.

12. These equations were programmed on an SD 80, 100-volt capacity analog computer for simulation of the desired obstacle tests. The analog flow diagram is shown in fig. A3 . The equations were scaled to meet the limits shown below.

| Variable | Limits |
|---|---|
| $\ddot{z}$ | ±2000 in./sec$^2$ |
| $\dot{z}$ | ±200 in./sec |
| $z$ | ±20 in. |
| $\ddot{\theta}$ $\ddot{\phi}$ | ±35 rad/sec$^2$ |
| $\dot{\theta}$ $\dot{\phi}$ | ±3.5 rad/sec |
| $\theta$ $\phi$ | ±0.35 rad |

13. The obstacles were implemented through use of digital logic circuits as shown by the diagram in fig. A4 , and had an appearance resembling that of semicircles.

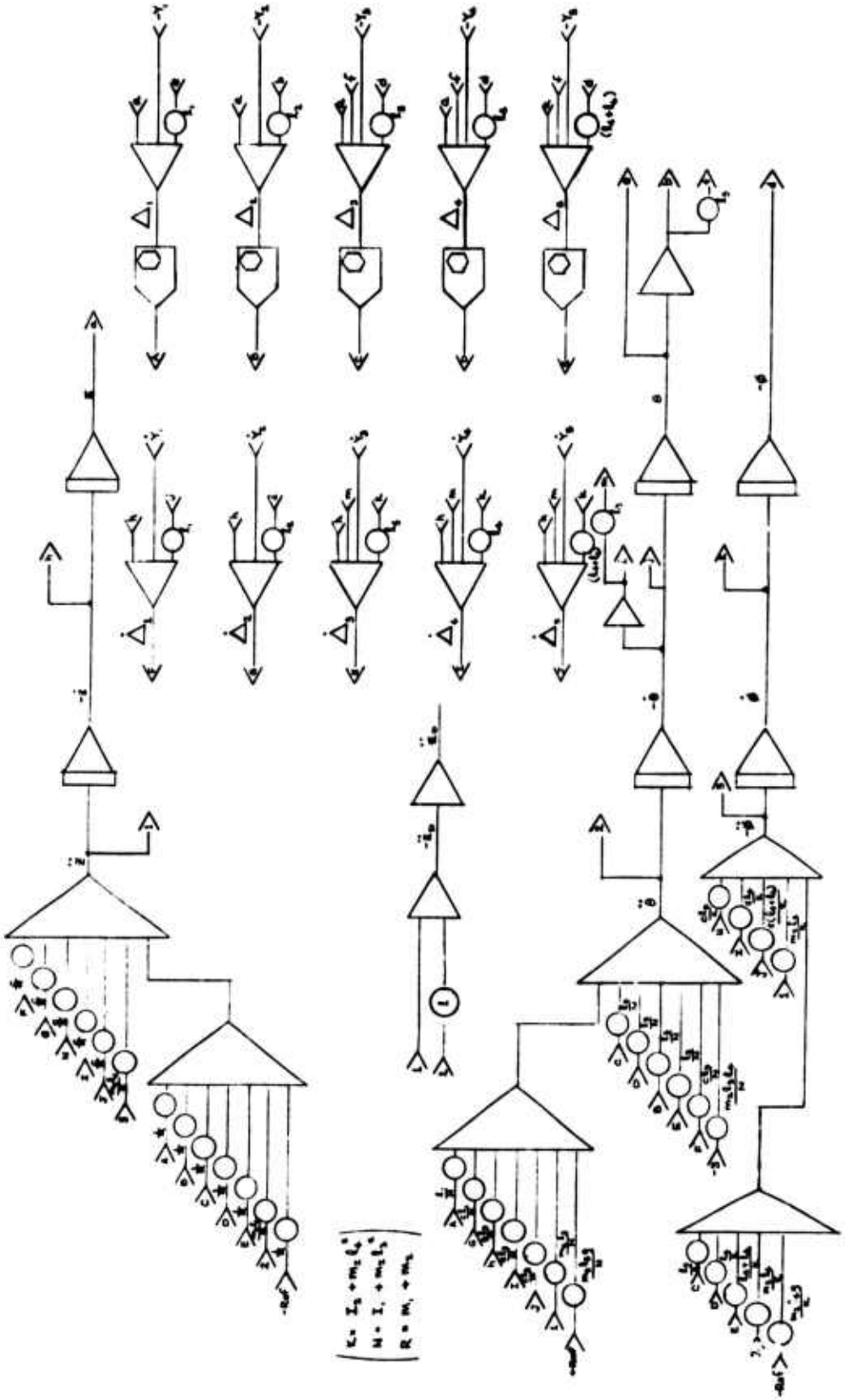

Fig. A3. Analog flow chart for MEXA 10x10 test bed

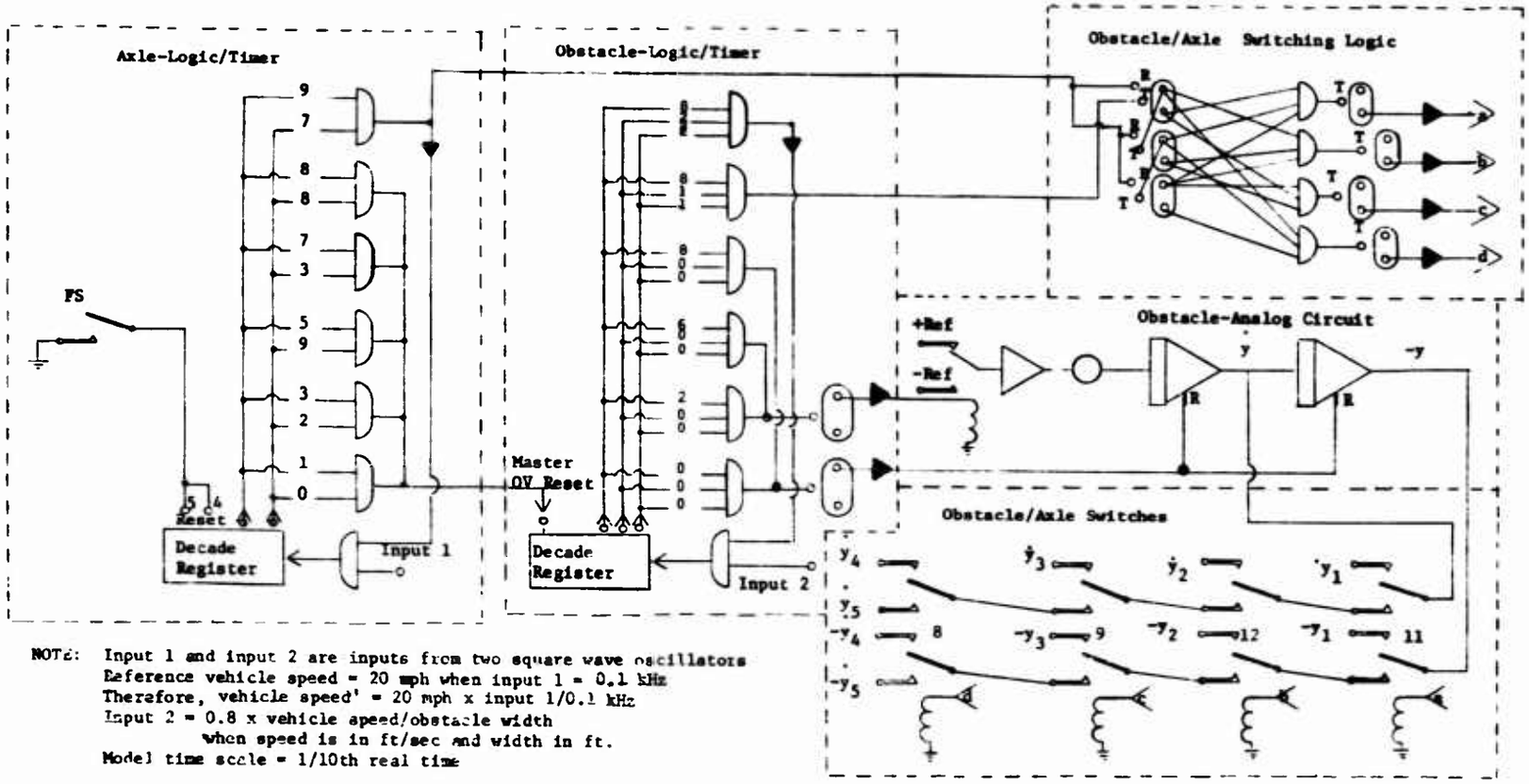


Fig. A4. Logic diagram for describing and positioning obstacles

## Digital Model of XM410E1

14. The dynamic responses of the XM410E1 while traversing single obstacles used in the field test program were predicted by a digital computer model consisting of a series of simultaneous differential equations of a mass-spring-damper representation. The equations used were developed for WES by FMC Corporation, Ordnance Engineering Division.[4*]

15. Certain changes in the original FMC computer program have evolved as a result of experience gained through application of the model. The changes that are of significance to this study are:

a. The small-angle assumption in the original model was altered to appropriately treat large rotational motions.

b. Time is the variable of integration. A correction to the code was made so that halving the integration-step size is possible. (When a suspension spring or damper-table value is exceeded by computation, the integration-step size is halved and the computation tried again. A minimum step size is entered as data and any attempt to go below this stops the program).

c. A limiting value of horizontal distance is entered as data. The integration of a particular problem will stop when either time or horizontal distance is exceeded.

d. The tire spring force is computed by summation of tire segments represented by linear springs.[5*] This representation allows the tire to envelop small obstacles without entering large forces into the system. Each tire has a set of spring constants so that variation in tire pressure or tire size may be modeled.

---

* See Literature Cited on page 21.

16. The program is designed so that any generalized vehicle assembly can be analyzed in terms of one basic computer program. The differential equations are programmed on a digital computer and solved using the Merson's modified Runge-Kutta numerical integration method. This integration scheme is extremely stable and uses a variable step size. For this study, the minimum step size was fixed at 0.007813 sec.

17. The program considers three degrees of freedom (bounce, pitch, and roll) for the vehicle body and two degrees of freedom (bounce and roll) for each of the axle assemblies. The initial conditions are established as part of the first "run" of the model, by allowing the vehicle to settle and reach equilibrium. This check of equilibrium conditions and the associated transient motions is often used as a guide in making minor adjustments in the vehicle characteristics, such as changes in the suspension damping to compensate for structural damping and frictional damping that are not specifically accounted for in the model. If data are available from vehicle tests conducted on natural irregular surfaces or prepared courses of single or multiple vertical obstacles, other adjustments in the model can be made to improve its accuracy. For example, it is often the case that minor adjustments in the body pitch moment of inertia, center of gravity, or masses will substantially improve the accuracy of the model in predicting actual measured responses. Such adjustments, in fact, are usually essential to obtain good validation of a vehicle dynamics model, since the majority of data readily available on the dynamic properties of a vehicle are seldom accurate enough to satisfy the model mathematics. Thus, model "tuning" is always required to obtain a high level of simulation accuracy.

18. Terrain geometry is described for the program as a series of x-y coordinates that is used as a table-look-up with linear interpolation by the computer to produce a continuous terrain forcing function. A schematic diagram illustrating the mass-spring-damper composition and sign convention for the generalized digital model is shown in fig. A5. A description of the basic axle and body motions for a generalized vehicle

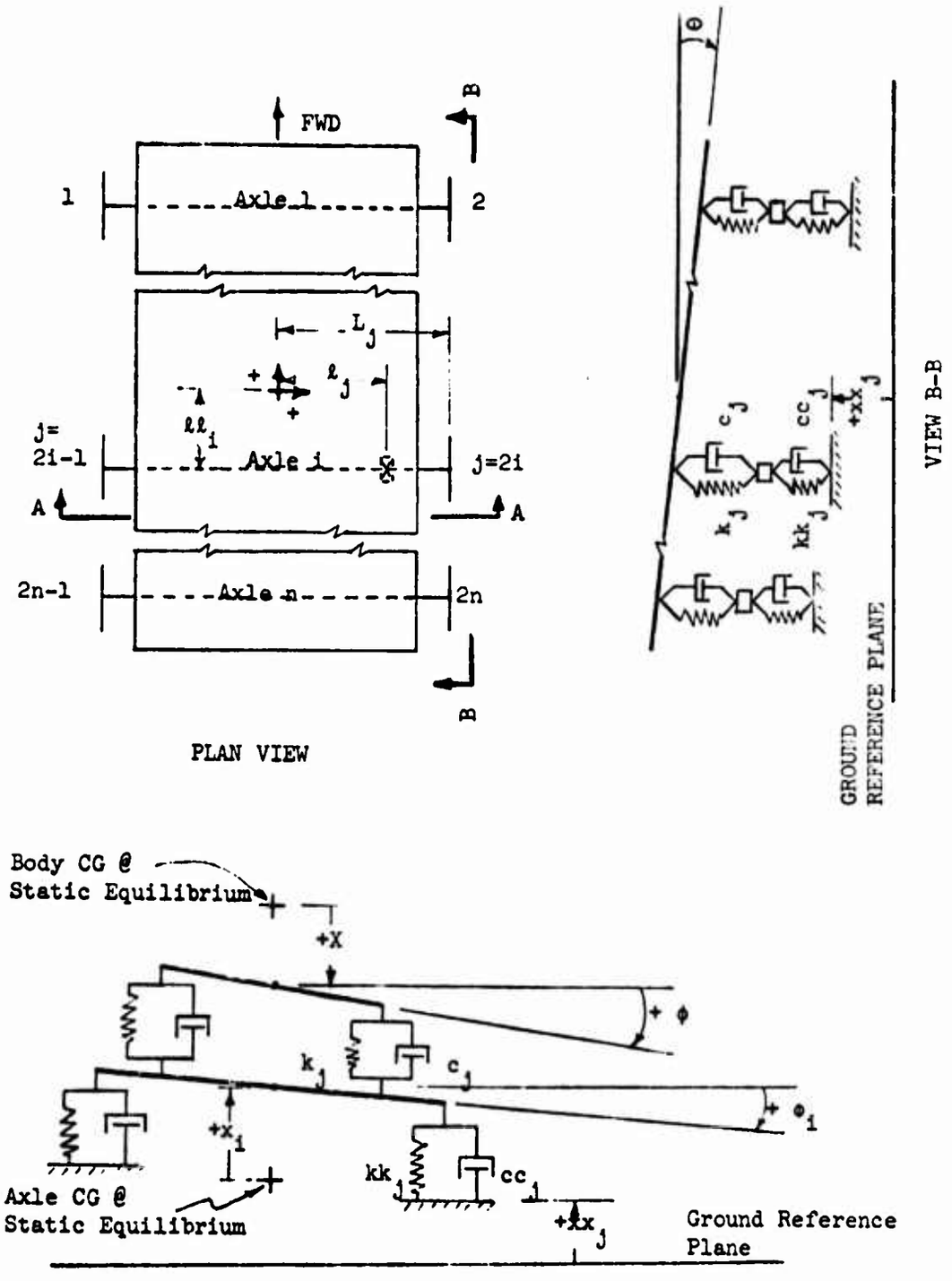


Fig. A5. Schematic of the generalized digital model illustrating the mass-spring-damper configuration and sign convention

is given in the following paragraphs. Input data for the XM410E1 used in the dynamic response model are listed in table A1.

Body bounce

19. The vertical bounce of the body of the vehicle with respect to its center of gravity is evaluated by one equation of motion that includes all spring, damping, and accelerating forces acting on the vehicle body. The positive forces are directed toward the ground.

Body pitch

20. The pitching motion of the vehicle body is described by one equation that is the sum of the vehicle's pitching moments with respect to the center of gravity of the vehicle. Positive pitching moments produce a nose-down condition for the vehicle. The equation includes all moments about the center of gravity due to pitching, angular accelerations, springs, and dampers.

Body roll

21. Rolling motion of the vehicle body is described by one equation that sums the rolling moments at the center of gravity of the vehicle. The equation includes rolling moments due to springs, dampers, and roll acceleration of the vehicle. Positive roll moments produce a right-side-down roll of the vehicle as it is viewed from the rear. In this study, predictions of dynamic response were made with the front wheels of the vehicle encountering the same obstacle at the same time, i.e. the obstacle was perpendicular to the direction of travel, thus essentially eliminating the effects due to roll motion.

Axle bounce

22. The program is capable of describing the motions of vehicles with as many as 10 axles--two equations for each axle, one for bounce and one for roll. The general equation that describes the vertical bounce of the axles is obtained by summing the total forces acting on the axle assembly due to acceleration, the wheels, and suspension springs and dampers. All positive displacements or forces are up.

Axle roll

23. One general equation describes the roll of the axle assemblies. This equation is obtained by summing the total rolling moments with respect to the center of gravity of the axle. This again generates one equation for each axle of the vehicle. The equations include all moments reacted by the axle due to the wheels, springs, dampers, and roll acceleration. A positive displacement is the right side down, when one views the vehicle from the rear. Axle roll did not affect the dynamic response predictions made in this study for the same reasons body roll was not an effect (paragraph 21).

Model output

24. The output of the dynamic response model includes computations of acceleration, velocity, and displacement for all degrees of freedom of the vehicle body, driver seat, and axle centers of gravity. Also obtainable are the vector sum of the vertical and longitudinal accelerations at the vehicle center of gravity and at the driver's seat. A detailed printout of all motions can be obtained as well as time history plots. The terrain profile plotted against time is used to correlate the vehicle's position on the terrain profile with displacement and acceleration responses.

Suspension characteristics

25. The nature of these tests, which minimized any effects of roll, permitted the use of a solid-axle model to suitably represent an independent suspension such as that on the XM410E1. The force-deflection and force-velocity relations used to characterize the spring damping rates of the suspensions are illustrated in figs. A6 and A7, respectively.

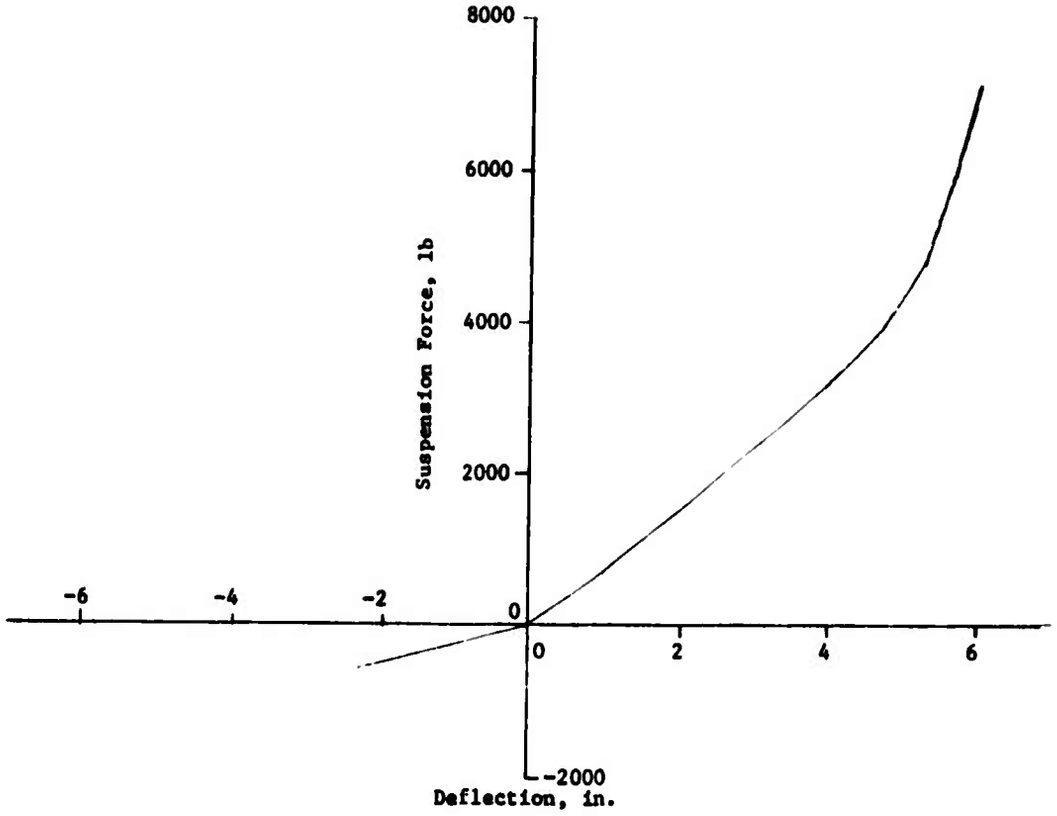


Fig. A6. Force-deflection relation for describing spring rate of XM410E1 suspension

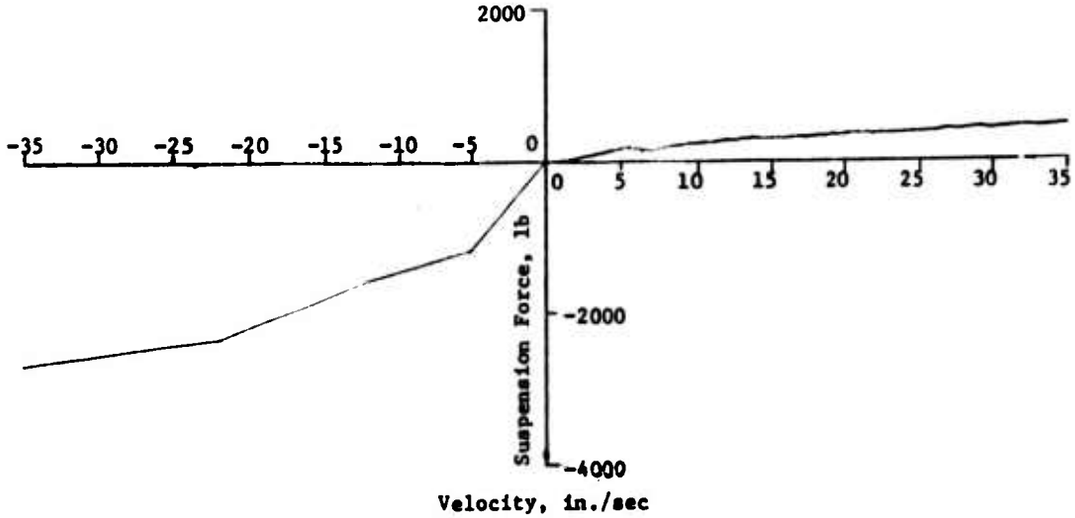


Fig. A7. Force-velocity relation for describing damping rate of XM410E1 suspension

Table A1

XM410E1 Input Parameters for Digital Dynamic Response Model

| Symbol | Description | Value |
|---|---|---|
| N | Number of axles | 4 |
| $\bar{X}_{1-8}$ | Height of axle CG above ground at full load, in. | |
| | Axles (front to rear) | |
| | No. 1 | 19.13 |
| | No. 2 | 19.13 |
| | No. 3 | 19.75 |
| | No. 4 | 19.75 |
| $\bar{X}$ | Height of body CG above ground at full load, in. | 41.8 |
| W | Sprung weight, lb | 12,900* |
| | Axle-to-body CG distance, in., wheel sets, front to rear | |
| $\ell\ell_1$ | No. 1 | 86.3 |
| $\ell\ell_2$ | No. 2 | 36.3 |
| $\ell\ell_3$ | No. 3 | 41.2 |
| $\ell\ell_4$ | No. 4 | 91.2 |
| $\ell_{1-8}$ | Suspension-to-longitudinal axis (body CG) distance, in. | 30.00 |
| $L_{1-8}$ | Wheel-to-longitudinal axis (body CG) distance, in. | 38.00 |
| $W_1$ | Unsprung weight of axle, lb (equal for all axles) | 900* |
| S | Spring suspension reference distance, in. (equal for all suspensions) | 27.23 |
| $R_{1-8}$ | Tire reference distance, in. (undeflected wheel radius) | 19.56 |
| $\bar{I}_y$ | Body pitch inertia, in.-lb/sec$^2$ | 260,000 |
| $\bar{I}$ | Body roll inertia, in.-lb/sec$^2$ | 42,000 |
| $\bar{I}_z$ | Axle roll inertia, in.-lb/sec$^3$ (equal for all axles) | 3,450 |
| | Accelerometer position-to-body CG distance, in. | |
| $D_1$ | Longitudinal | 88.8 front |
| $D_2$ | Vertical | 4.65 up |
| $D_3$ | Lateral | 39.0 left |

(Continued)

* Estimated.

Table A1 (Concluded)

| Symbol | Description | Value |
|---|---|---|
| $K_j$ | Torsion bar force versus deflection, lb/in. (equal for all suspensions) | [see fig. A5] |
| $C_j$ | Shock absorber force versus velocity, lb-sec/in. | [see fig. A5] |
| $KK_j$ | Tire spring of segmented wheel - 12 seg at 10°, lb/in. | 530.00* |
| $CC_j$ | Tire damping rate, lb-sec/in. | 3.14* |

* Assumed to be linear.

Unclassified
Security Classification

**DOCUMENT CONTROL DATA - R & D**

*(Security classification of title, body of abstract and indexing annotation must be entered when the overall report is classified)*

1. ORIGINATING ACTIVITY *(Corporate author)*

U. S. Army Engineer Waterways Experiment Station
Vicksburg, Mississippi

2a. REPORT SECURITY CLASSIFICATION

Unclassified

2b. GROUP

3. REPORT TITLE

MOBILITY EXERCISE A (MEXA) FIELD TEST PROGRAM; Report 4, PERFORMANCE OF SELECTED MEXA AND MILITARY VEHICLES IN VERTICAL OBSTACLES

4. DESCRIPTIVE NOTES *(Type of report and inclusive dates)*

Report 4 of a series

5. AUTHOR(S) *(First name, middle initial, last name)*

Newell R. Murphy, Jr.
Adam A. Rula

| 6. REPORT DATE | 7a. TOTAL NO. OF PAGES | 7b. NO. OF REFS |
|---|---|---|
| January 1974 | 62 | 5 |

| 8a. CONTRACT OR GRANT NO. | 9a. ORIGINATOR'S REPORT NUMBER(S) |
|---|---|
| b. PROJECT NO 1T162112A131 and 1T162112A046 | Technical Report M-70-11, Report 4 |
| c. Task 02 | 9b. OTHER REPORT NO(S) *(Any other numbers that may be assigned this report)* |
| d. | |

10. DISTRIBUTION STATEMENT

Approved for public release; distribution unlimited.

| 11. SUPPLEMENTARY NOTES | 12. SPONSORING MILITARY ACTIVITY |
|---|---|
| | U. S. Army Materiel Command<br>Washington, D. C. |

13. ABSTRACT

Fifty tests were conducted with two vehicles, an XM410E1, 8x8, 2-1/2-ton cargo truck and the MEXA 10x10, 2-1/2-ton, wheeled, articulated test bed. The vertical obstacle test course at WES, on which rigid, single or multiple obstacles of various heights and shapes can be tested, was used. The primary purpose of these tests was to obtain data to relate obstacle height, vehicle speed, and vertical acceleration (at selected locations on the vehicle) for use as input to the AMC-71 cross-country mobility prediction model. A secondary purpose was to provide data for use in verifying the vehicle dynamics prediction models using test data for the XM410E1 and MEXA 10x10. Results of the test are presented by curves relating, for a series of obstacle heights, the speed of the vehicle at contact with the obstacle versus peak accelerations at selected locations on the vehicle, and obstacle height versus speed for a vertical acceleration of 2.5 g's in the driver's compartment and vehicle center of gravity. Test data are compared with predicted results obtained from the dynamic response computer models for both vehicles. The results indicate among other things that: (a) the intensity of vertical acceleration depends on the location in the vehicle; (b) human tolerance levels are reached only for vertical accelerations; (c) tire pressure can significantly affect peak acceleration relations; (d) for a given level of acceleration, speed decreases with an increase in obstacle height; and (e) with proper input the mathematical models can be used to adequately simulate speed-obstacle height relations. It is recommended that additional data be obtained for a variety of vehicle types to establish experimental speed-obstacle height relations to determine if peak vertical accelerations and obstacle heights are suitable quantities for defining obstacle-crossing capabilities, and to validate the current models that simulate dynamic response.

DD FORM 1 NOV 68 1473 REPLACES DD FORM 1473, 1 JAN 64, WHICH IS OBSOLETE FOR ARMY USE.

Unclassified
Security Classification

| 14. KEY WORDS | LINK A | | LINK B | | LINK C | |
|---|---|---|---|---|---|---|
| | ROLE | WT | ROLE | WT | ROLE | WT |
| Field tests | | | | | | |
| MEXA (Mobility Exercise A) test program | | | | | | |
| Military vehicles | | | | | | |
| Mobility | | | | | | |
| Obstacles | | | | | | |

In accordance with ER 70-2-3, paragraph 6c(1)(b), dated 15 February 1973, a facsimile catalog card in Library of Congress format is reproduced below.

Murphy, Newell R

Mobility Exercise A (MEXA) field test program; report 4: Performance of selected vertical MEXA and military vehicles in vertical obstacles, by N. R. Murphy, Jr. and A. A. Rula. Vicksburg, U. S. Army Engineer Waterways Experiment Station, 1974.

1 v. (various pagings) illus. 27 cm. (U. S. Waterways Experiment Station. Technical report M-70-11, Report 4)

Sponsored by U. S. Army Materiel Command, Washington, D. C., Projects No. 1T162112A131 and No. 1T162112A046, Task 02.

Includes bibliography.

1. Field tests. 2. MEXA (Mobility Exercise A) test program. 3. Military vehicles. 4. Mobility. 5. Obstacles. I. Rula, Adam A., joint author. II. U. S. Army Materiel Command. (Series: U. S. Waterways Experiment Station, Vicksburg, Miss. Technical report M-70-11, Report 4)
TA7.W34 no.M-70-11 Report 4